Mimetic finite differences for nonlinear and control problems

P. F. Antonietti

MOX–Dipartimento di Matematica,
Politecnico di Milano,
P.zza Leonardo da Vinci 32, 20133 Milano, Italy
paola.antonietti@polimi.it

L. Beirão da Veiga

Dipartimento di Matematica,
Università degli Studi di Milano,
Via Saldini 50, I-20133 Milano, Italy
lourenco.beirao@unimi.it

N. Bigoni* and M. Verani†

MOX–Dipartimento di Matematica,
Politecnico di Milano,
P.zza Leonardo da Vinci 32, 20133 Milano, Italy
**nadia.bigoni@polimi.it*
†marco.verani@polimi.it

Received 7 March 2013
Revised 28 June 2013
Accepted 11 December 2013
Published 24 February 2014
Communicated by F. Brezzi and G. Manzini

*Corresponding author

1. Introduction

Nowadays, the mimetic finite difference (MFD) method has become a very popular numerical approach to successfully solve a wide range of problems. This is undoubtedly connected to its great flexibility in dealing with very general polygonal meshes and its capability of preserving the fundamental properties of the underlying physical and mathematical models. The MFD method has been applied with success to a wide range of *linear* problems, such as the diffusion problem in mixed[36–39] and primal form,[20,32] linear elasticity,[13] the Stokes equations,[17–19] Reissner–Mindlin plate equations,[22,24] electromagnetics,[31,33] convection–diffusion problems,[16,44] eigenvalue problems,[42] modeling of biological suspensions,[72] modeling of flows in porous media,[93] acoustic equation.[71] Issues and techniques such as satisfaction of maximum principle,[91,92] *a posteriori* error estimation[3,12,23] and solution post-processing[43] have been also considered. We refer the interested reader to the recent review paper[90] and the book[21] for a more detailed introduction of the MFD method. Recently, in Ref. 14, the mimetic approach has been recasted as the *virtual element method*, see also Refs. 15 and 40. Nevertheless, the application of the MFD method to *nonlinear* problems is even more recent.

Nonlinear and control problems play an important role in applied mathematics and engineering. They have been extensively used to model phenomena in a wide range of applications including fluid dynamics, biology, and materials science, for example. The application we have in mind is the extrusion manufacturing process, one of the most important manufacturing processes employed in industry. Extrusion is a manufacturing process where a raw (plastic, metal or foodstuffs) material is melted and pushed through a die to obtain an object with the desired cross-sectional profile. A wide range of objects are produce by extrusion: pipes, textiles, rails, and pasta, for example.

The aim of this paper is to review some recent applications of the MFD method to nonlinear problems (variational inequalities and quasilinear elliptic equations) and constrained control problems governed by linear elliptic partial differentail equations (PDEs). In particular, we will show through several numerical examples the efficacy of MFDs in building accurate numerical approximations. This is of paramount importance due to the ubiquitous presence of nonlinear and control problems in applied and industrial problems.

The outline of the paper is the following. In Sec. 2 we collect some useful notation and assumptions that will be employed throughout the paper. In Sec. 3 we consider the MFD approximation of the obstacle problem, a paradigmatic example of variational inequality, while in Sec. 4 we consider the performance of the MFD method in approximating quasilinear elliptic problems. In Sec. 5 we turn the attention to the mimetic approximation of optimal control problems governed by linear elliptic equations. Finally, in Sec. 6, motivated by the numerical simulation of the industrial extrusion process, we explore further applications of the MFD method to nonlinear Stokes equations and shape optimization/free-boundary problems, while in Sec. 7 we draw some conclusions.

2. Mesh Assumptions and Degrees of Freedom

The aim of this section is to introduce some notation and the mesh assumptions, and to define the degrees of freedom for the discrete approximation spaces we are going to introduce later on. Throughout the paper, we will follow the usual notation for Sobolev spaces and norms (see e.g. Ref. 49). Moreover, for any subset $\mathcal{D} \subseteq \mathbb{R}^2$ and non-negative integer k, we indicate by $\mathbb{P}_k(\mathcal{D})$ the space of polynomials of degree up to k defined on $\mathcal{D}$. Finally, we will use the symbol $\lesssim$ to indicate an upper bound that holds up to a positive multiplicative constant independent of h.

2.1. *Mesh assumptions*

Let Ω be a regular enough two-dimensional domain, and let Ω_h be a non-overlapping partition of Ω into, possibly non-convex, polygonal elements E with granularity $h = \sup_{E \in \Omega_h} h_E$, being h_E the diameter of $E \in \Omega_h$. We denote by $\mathcal{N}_h^\circ$ and $\mathcal{N}_h^\partial$ the sets of interior and boundary mesh vertices, respectively, and set $\mathcal{N}_h = \mathcal{N}_h^\circ \cup \mathcal{N}_h^\partial$. Proceeding as in Ref. 32 we also assume the following.

Assumption 2.1. (Mesh regularity assumptions) There exist an integer number N and a shape regularity constant, both independent of h, such that for every element $E \in \Omega_h$ there exists a compatible sub-decomposition $\mathcal{T}_h^E$ with at most N *shape-regular* triangles.

We point out that Assumption 2.1 only requires the existence of a *compatible* sub-mesh that does not have to be constructed in practice. Moreover, it is easy to check that Assumption 2.1 guarantees that the following mesh regularity properties are satisfied:

(i) There exists $N_\mathsf{e} > 0$ such that every element E has at most N_e edges;
(ii) There exists $\gamma > 0$ such that for every element E and for every edge e of E, it holds $|\mathsf{e}| \geq \gamma h_E$, where $|\mathsf{e}|$ is the length of e;
(iii) For every $E \in \Omega_h$ and for every edge e of E, the following *trace inequality* holds

$$\|\psi\|^2_{L^2(\mathsf{e})} \lesssim h_E^{-1} \|\psi\|^2_{L^2(E)} + h_E \, |\psi|^2_{H^1(E)} \qquad \forall\, \psi \in H^1(E).$$

2.2. *Degrees of freedom for scalar and vector fields*

In the following we will require to discretize scalar fields in $H^1(\Omega)$ and $L^2(\Omega)$, as well as vector fields in $H(\mathrm{div}, \Omega)$. Therefore, the scope of this section is to introduce the corresponding finite-dimensional spaces V_h, Q_h, and X_h together with suitable interpolation operators from the continuous spaces to the associated discrete ones, and set up some notation.

We start defining the finite-dimensional space V_h aiming at approximating the elements of $H^1(\Omega)$. Every discrete function $v_h \in V_h$ is a vector of real components $v_h = \{v^\mathsf{v}\}_{\mathsf{v} \in \mathcal{N}_h}$ one per mesh vertex, so that the dimension of V_h equals to the numbers of vertices of the mesh Ω_h. We also define V_h^g as the subset of V_h consisting of functions satisfying a Dirichlet-type boundary condition

$$V_h^g = \{v_h \in V_h : v_h^{\mathsf{v}} = g(\mathsf{v}) \ \forall \mathsf{v} \in \mathcal{N}_h^\partial\},$$

with g a given smooth enough function. Accordingly, V_h^0 represents the space of discrete functions vanishing at the boundary nodes.

The space V_h is endowed with the following discrete seminorm:

$$\|v_h\|_{1,h}^2 = \sum_{E\in\Omega_h} \|v_h\|_{1,h,E}^2 = \sum_{E\in\Omega_h} |E| \sum_{\substack{\mathsf{e}\in\mathcal{E}_h \\ \mathsf{e}\subset\partial E}} \left[\frac{1}{|\mathsf{e}|}(v^{\mathsf{v}_2} - v^{\mathsf{v}_1})\right]^2, \tag{2.1}$$

which becomes a norm in V_h^0. Here v_1 and v_2 are the two endpoints of $\mathsf{e} \in \mathcal{E}_h$, and $|E|$ is the area of the element $E \in \Omega_h$.

We define the following interpolation operator from the space $\mathcal{C}^0(\bar\Omega) \cap H^1(\Omega)$ into the discrete space V_h. For any $v \in \mathcal{C}^0(\bar\Omega) \cap H^1(\Omega), v_{\mathrm{I}} \in V_h$ is defined as

$$v_{\mathrm{I}}^{\mathsf{v}} = v(\mathsf{v}) \quad \forall \mathsf{v} \in \mathcal{N}_h. \tag{2.2}$$

Notice that, under Assumption 2.1, the above interpolation operator satisfies classical approximation estimates, see Ref. 4. The local version of the operator (2.2) is defined accordingly. That is, for any $v \in \mathcal{C}^0(\bar E) \cap H^1(E), v_{\mathrm{I}} \in V_h|_E$ is given by

$$v_{\mathrm{I}}^{\mathsf{v}} = v(\mathsf{v}) \quad \forall \mathsf{v} \in \mathcal{N}_h^E,$$

with $\mathcal{N}_h^E$ the set of vertices of the polygon $E \in \Omega_h$.

Next we introduce the discrete space Q_h describing the degrees of freedom associated to a scalar field in $L^2(\Omega)$. Every discrete function $q_h \in Q_h$ is a vector of real components one per mesh cell, so that the dimension of Q_h equals the number of polygons in Ω_h. That is, for $q_h \in Q_h$ we have $q_h = \{q_E\}_{E\in\Omega_h}$, with $q_E \in \mathbb{R}$ the value of the discrete variable associated to the polygon $E \in \Omega_h$.

We endowed Q_h by the following scalar product

$$[p_h, q_h]_{Q_h} = \sum_{E\in\Omega_h} |E| p_E q_E \quad \forall p_h,\ q_h \in Q_h, \tag{2.3}$$

and denote by $\|\cdot\|_{Q_h}$ the induced norm, i.e.

$$\|p_h\|_{Q_h}^2 = [p_h, p_h]_{Q_h} \quad \forall p_h \in Q_h. \tag{2.4}$$

Notice that (2.3) coincide with the $L^2(\Omega)$ scalar product for piecewise constant functions.

For further use, we also introduce the following operator from $L^1(\Omega)$ onto Q_h

$$q_{\mathrm{I}}|_E = \frac{1}{|E|}\int_E q\, dV \quad \forall E \in \Omega_h,\ \forall q \in L^1(\Omega). \tag{2.5}$$

Finally, we introduce the finite-dimensional space X_h aiming at approximating the elements of $H(\mathrm{div}, \Omega)$. In order to completely describe a vector field $G_h \in X_h$, we associate to any mesh edge $\mathsf{e} \in \mathcal{E}_h$ a real number $G_{\mathsf{e}} \in \mathbb{R}$, so that for $G_h \in X_h$, we have $G_h = \{G_{\mathsf{e}}\}_{\mathsf{e}\in\mathcal{E}_h}$. Clearly, the dimension of X_h is equal to the cardinality of $\mathcal{E}_h$.

The scalar product in X_h is defined by assembling elementwise contributions from each element, i.e.

$$[F_h, G_h]_{X_h} = \sum_{E\in\Omega_h} [F_h, G_h]_E \quad \forall\, F_h,\;\; G_h \in X_h, \tag{2.6}$$

where the precise definition of $[\cdot,\cdot]_E$ will made be clear later on. The space X_h is equipped with the induced norm i.e.

$$\|F_h\|^2_{X_h} = [F_h, F_h]_{X_h} \quad \forall\, F_h \in X_h.$$

For any edge $\mathsf{e} \in \mathcal{E}_h$, we denote by $\mathbf{n}_{\mathsf{e}}$ the unit normal vector to $\mathsf{e} \in \mathcal{E}_h$ fixed once and for all, and define the projection operator from $H(\mathrm{div},\Omega)\cap[L^s(\Omega)]^2$, $s > 2$, onto X_h as follows:

$$G_{\mathrm{I}}|_{\mathsf{e}} = \frac{1}{|\mathsf{e}|}\int_{\mathsf{e}} G\cdot\mathbf{n}_{\mathsf{e}}\, dS \quad \forall\,\mathsf{e}\in\mathcal{E}_h \quad \forall\, G \in H(\mathrm{div},\Omega). \tag{2.7}$$

Finally, we define the discrete divergence operator form, the space X_h onto Q_h,

$$\begin{gathered}\mathcal{DIV}_h : X_h \to Q_h,\\ \mathcal{DIV}_h(G_h)|_E = \frac{1}{|E|}\sum_{\mathsf{e}\subseteq\partial E} |\mathsf{e}| G^E_{\mathsf{e}} \quad \forall\, E\in\Omega_h,\end{gathered} \tag{2.8}$$

where $G^E_{\mathsf{e}} = G_{\mathsf{e}}\mathbf{n}_{\mathsf{e}}\cdot\mathbf{n}^E_{\mathsf{e}} \in \mathbb{R}$ and $\mathbf{n}^E_{\mathsf{e}}$ is the unit normal vector to e pointing outward to $E \in \Omega_h$. It is immediate to check that $\mathcal{DIV}_h(G_I) = (\mathrm{div}\, G)_I$ for all sufficiently regular vector fields G, where the first interpolation is in X_h and the second in Q_h.

The local bilinear forms (2.6) are defined as in Ref. 36 and satisfy the following two conditions:

(S1) *Continuity and coercivity*: For any $E \in \Omega_h$, it holds

$$\sum_{\mathsf{e}\subseteq\partial E} |E|(G^E_{\mathsf{e}})^2 \lesssim [G_h, G_h]^2_E \lesssim \sum_{\mathsf{e}\subseteq\partial E} |E|(G^E_{\mathsf{e}})^2 \quad \forall\, G_h \in X_h.$$

(S2) *Local consistency*: For every linear function q^1 on $E \in \Omega_h$, it holds

$$[(\nabla q^1)_{\mathrm{I}}, G_h]_E + \int_E q^1\, \mathcal{DIV}_h(G_h)\, dV = \sum_{\mathsf{e}\subseteq\partial E} G^E_{\mathsf{e}} \int_{\mathsf{e}} q^1\, dS \quad \forall\, G_h \in X_h.$$

3. The Obstacle Problem

The goal of this section is to show that MFD methods can be successfully applied to discretize variational inequalities. To this aim we consider the simplest example, namely the obstacle problem, which consists in finding the equilibrium position of an elastic membrane whose boundary is held fixed, and which is constrained to lie above a given obstacle. In Sec. 3.1 we recall the continuous problem, then Sec. 3.2

is devoted to present the MFD discretization and the approximation results and finally Sec. 3.3 presents some numerical computations. In the sequel, we will assume that the computational domain Ω is an open, bounded, convex set of $\mathbb{R}^2$, with either a polygonal or a C^2-smooth boundary.

3.1. *Problem and literature*

The elliptic obstacle problem can be considered as a model problem for variational inequalities (see e.g. Ref. 67), and it has found applications in a number of different fields as elasticity and fluid dynamics. For example, applications include fluid filtration in porous media, optimal control, and financial mathematics.[83,86]

The problem is written as follows. Let $\psi \in H^2(\Omega)$ be a given function that satisfies $\psi \leq g$ on $\partial\Omega$, where g is the trace of a given function in $H^2(\Omega)$, and let K be the convex set defined as

$$K = \{v \in H^1(\Omega) : v = g \text{ on } \partial\Omega \text{ and } \ v \geq \psi \text{ a.e. in } \Omega\}.$$

The obstacle problem can be written as the following variational inequality:

$$\text{Find } u \in K \text{ such that } a(u, v-u) \geq F(v-u) \quad \forall v \in K, \tag{3.1}$$

where the bilinear form $a(\cdot,\cdot) : H^1(\Omega) \times H^1(\Omega) \to \mathbb{R}$ and the linear functional $F(\cdot) : H^1(\Omega) \to \mathbb{R}$ are defined as

$$a(u,v) = \int_\Omega \nabla u \cdot \nabla v dV, \quad F(v) = \int_\Omega f v dV, \tag{3.2}$$

respectively, with $f \in L^2(\Omega)$ a given function. It can be shown that under the above data regularity assumption, the elliptic obstacle problem (3.1) admits a unique solution $u \in H^2(\Omega)$, see e.g. Ref. 30 and Corollary 5:2.3 in Ref. 109.

The finite element analysis of problem (3.1) dates back to the seventies. In Ref. 60 the author develops a theoretical analysis for the method that is valid for a general class of variational inequalities and is then applied to the elliptic obstacle problem. Following a different technique, in Ref. 34 the authors develop an optimal convergence result of order $O(h)$ for linear elements and order $O(h^{3/2-\varepsilon})$ for quadratic elements. In Ref. 35, optimal error bounds are proved also for the mixed finite element discretization of the obstacle problem. In Ref. 118 the result of Ref. 34 for quadratic elements is slightly improved by abandoning the "free-boundary finite length" hypothesis.

Another classical finite element approach to the problem, that must be mentioned, is that of using penalty formulations to enforce the obstacle constraint. This approach can be found in the early work,[85] where a convergence result is obtained by showing that the penalized solution converges (when the penalty parameter goes to zero) to the discrete solution of the mixed method in Ref. 35. Numerical results for the penalty method can be found in Ref. 112, while in Ref. 113 the time-dependent case was also investigated.

An area of research that received a lot of attention in the literature is that of *a posteriori* error estimation for the obstacle problem. In Ref. 1 *a posteriori* error indicators are obtained by using the dual principle, while Ref. 78 uses a combination of the primal and dual formulation. In Ref. 47, by using an *ad hoc* interpolation operator that requires minimal regularity, the authors analyze a new residual-based error estimator. Sharp *a priori* bounds for the estimator are also provided. In Ref. 116 it is developed a new approach to obtain *a posteriori* error estimators without resorting to the positivity preserving interpolation of Ref. 47. In Ref. 28 the author shows that the error estimation of the obstacle problem can be derived with arguments that are rather near to the standard ones for the linear case. In Ref. 11 a gradient-averaging type of error estimator for the finite element obstacle problem is introduced and shown to be reliable and efficient. Furthermore, in Ref. 29 an error estimator based on jump contributions of standard residuals is developed and combined with an adaptive strategy. A theoretical analysis is also shown for the case of a model obstacle problem. *A posteriori* error indicators of hierarchical type have been proposed and analyzed in Refs. 80 and 88 and more recently in Refs. 114 and 124. Regarding the *a posteriori* error analysis for the penalty formulation of the obstacle problem, we mention the seminal work[84] where an *a posteriori* upper bound is obtained under the hypothesis $\psi = 0$. Later studies have been carried out in Refs. 66 and 26. In the first work, an error estimator for the maximum norm is proposed and analyzed. Such estimator is applicable both in the case of smooth but also rough obstacles. In the second paper an *a posteriori* error indicator in maximum norm for the time-dependent problem is investigated.

3.2. *Discrete problem and convergence*

We denote by $a_h(\cdot,\cdot) : V_h \times V_h \to \mathbb{R}$ the discretization of the bilinear form $a(\cdot,\cdot)$, defined as follows:

$$a_h(v_h, w_h) = \sum_{E\in\Omega_h} a_h^E(v_h, w_h) \quad \forall\, v_h,\ \ w_h \in V_h, \tag{3.3}$$

where $a_h^E(\cdot,\cdot) : V_h|_E \times V_h|_E \to \mathbb{R}$ are symmetric bilinear forms built on each element $E \in \Omega_h$ in such a way that the following properties are satisfied (see Ref. 32):

(S1) *Continuity and coercivity*: For every $u_h, v_h \in V_h$ and each $E \in \Omega_h$, we have

$$\|v_h\|^2_{1,h,E} \lesssim a_h^E(v_h, v_h), \quad a_h^E(u_h, v_h) \lesssim \|u_h\|_{1,h,E}\|v_h\|_{1,h,E}.$$

(S2) *Local consistency*: For every element E, every function $q^1 \in \mathbb{P}^1(E)$, and every $v_h \in V_h$, it holds

$$a_h^E(v_h, (q^1)_{\mathrm{I}}) = \sum_{\mathsf{e}\in\mathcal{E}_h^E} (\nabla q^1 \cdot \mathbf{n}_E^{\mathsf{e}}) \frac{|\mathsf{e}|}{2}(v_h^{\mathsf{v}_1} + v_h^{\mathsf{v}_2}),$$

where v_1 and v_2 are the two vertices of $\mathsf{e} \in \mathcal{E}_h$.

The meaning of the above consistency condition (S2) is that the discrete bilinear form respects integration by parts when tested with linear functions. The discretization of the load term is defined as

$$(f, v_h)_h = \sum_{E \in \Omega_h} \bar{f}|_E \sum_{i=1}^{k_E} v^{\mathsf{v}_i} \omega_E^i, \tag{3.4}$$

where $\mathsf{v}_1, \ldots, \mathsf{v}_{k_E}$ are the vertices of $E, \omega_E^1, \ldots, \omega_E^{k_E}$ are positive weights such that $\sum_{i=1}^{k_E} \omega_E^i = |E|$, and

$$\bar{f}|_E = \frac{1}{|E|} \int_E f dV.$$

Finally, we are able to define the proposed MFD method for the obstacle problem (3.1). Indeed, let us introduce the discrete convex space

$$K_h = \{v_h \in V_h^g : v_h^{\mathsf{v}} \geq \psi(\mathsf{v}) \ \forall \mathsf{v} \in \mathcal{N}_h\};$$

then the mimetic discretization of problem (3.1) reads as follows:

$$\text{Find } u_h \in K_h \text{ such that } a_h(u_h, v_h - u_h) \geq (f, v_h - u_h)_h \quad \forall\, v_h \in K_h. \tag{3.5}$$

It can be shown that problem (3.5) admits a unique solutions. Indeed, from property (S1), it is immediate to infer that the bilinear form $a_h(\cdot,\cdot)$ is coercive on $V_h/\mathbb{R}$. Then, the well posedness of (3.5) follows recalling that $K_h \subset V_h$ is convex and closed, and using standard results.[49] The following convergence result has been proved in Ref. 4.

Theorem 3.1. *Let $u \in K \cap H^2(\Omega)$ be the solution to the continuous problem* (3.1), *and $u_h \in K_h$ be the corresponding mimetic approximation obtained by solving the discrete problem* (3.5). *Then, it holds*

$$\|u_h - u_I\|_{1,h} \lesssim h.$$

3.3. *Numerical results*

We set $\Omega = (-1, 1)^2$ and consider a variant of the example presented in Ref. 4. Let $\psi(x, y) = 0$, and choose as exact solution of model problem (3.1)

$$u(x, y) = (\max\{x^2 + y^2 - r^2, 0\})^2, \tag{3.6}$$

with $r \in (0, 1)$ a parameter at our disposal. Figure 1 depicts the minimizer u given in (3.6) together with the obstacle ψ in the case $r = 0.3$. The corresponding load $f(\cdot,\cdot)$ is given by

$$f(x, y) = \begin{cases} -8(2x^2 + 2y^2 - r^2) & \text{if } \sqrt{x^2 + y^2} > r, \\ -8r^2(1 - x^2 - y^2 + r^2) & \text{if } \sqrt{x^2 + y^2} \leq r, \end{cases}$$

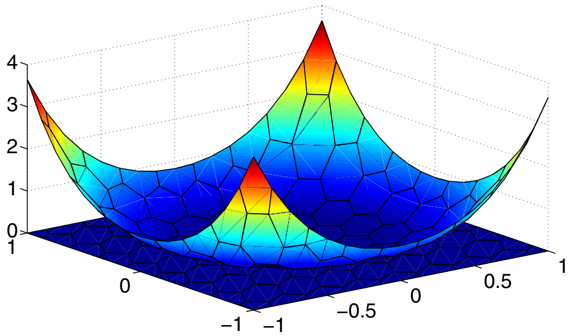

Fig. 1. Obstacle problem. Exact solution u given in (3.6), $r = 0.3$, and the obstacle $\psi = 0$.

and the Dirichlet boundary data $g(x, y) = (x^2 + y^2 - r^2)^2$. The obstacle problem (3.1) has been solved numerically by the Projected Successive Over Relaxation method (see Ref. 4 for more implementation details).

We have considered sequences of *quadrilateral*, *median-type* 1 and *median-type* 2 of decompositions as those shown in Fig. 2 for the first three refinement levels $\ell = 1, 2, 3$. In Table 1 we report the errors $\|u_{\mathrm{I}} - u_h\|_{1,h}$ measured in the discrete energy norm defined in (2.1) for the considered sequence decompositions. In the

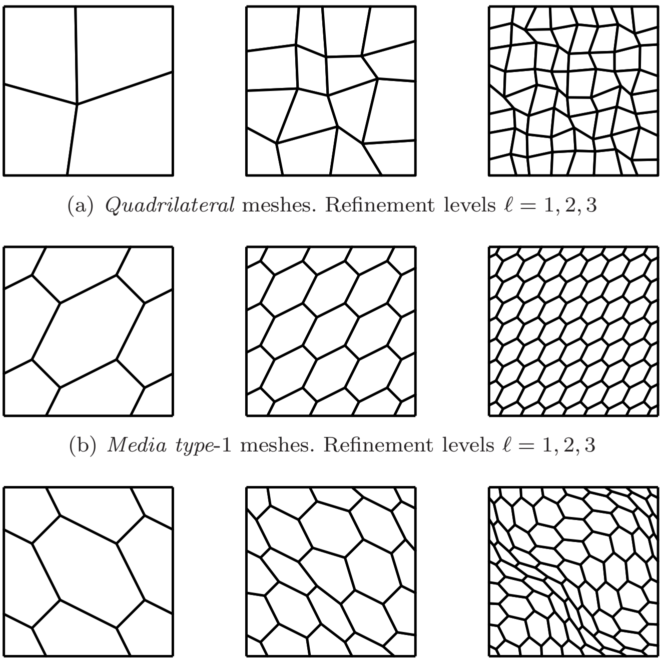

(a) *Quadrilateral* meshes. Refinement levels $\ell = 1, 2, 3$

(b) *Media type*-1 meshes. Refinement levels $\ell = 1, 2, 3$

(c) *Media type*-2 meshes. Refinement levels $\ell = 1, 2, 3$

Fig. 2. Samples of *quadrilateral*, *median-type* 1 and *median-type* 2 decompositions of $\Omega = (-1, 1)^2$. From left to right: refinement levels $\ell = 1, 2, 3$.

Table 1. Obstacle problem. Computed errors $\|u_{\mathrm{I}} - u_h\|_{1,h}$ on the sequence of *quadrilateral*, *median-type* 1 and *median-type* 2 decompositions.

Refinement level	*Quadrilateral*	*Median-type* 1	*Median-type* 2
$\ell = 1$	6.67435e−2	1.57514e−1	1.57514e-01
$\ell = 2$	6.04445e−2	6.71848e−2	6.20040e-02
$\ell = 3$	2.18688e−2	4.99534e−2	4.36785e-02
$\ell = 4$	1.04561e−2	2.55444e−2	1.95246e-02
$\ell = 5$	5.15400e−3	1.05753e−2	7.49375e-3
Rate	0.99210	1.02879	1.04544

last row of Table 1 we also report the computed convergence rates obtained by the linear regression algorithm. We can observe that on all the sequences of meshes a linear convergence rate is observed as predicted by Theorem 3.1. We refer to Ref. 5 for more numerical experiments including the numerical performance of an adaptive MFD method driven by a hierarchical *a posteriori* error estimator similar to the one proposed in Ref. 3.

4. Quasilinear Elliptic Problems

The aim of this section is to show that the MFD method can be successfully employed to discretize quasilinear elliptic equations. In Sec. 4.1, we will recall the model problem under investigation. In Sec. 4.2 we present the MFD discretization and the theoretical results that will also be validated by means of numerical experiments presented in Sec. 4.3.

4.1. *Problem and literature*

In this section, we discuss the application of the MFD method for the approximation of the following quasilinear elliptic problem: Find $u \in H_0^1(\Omega)$ such that

$$b(u; u, v) = F(v) \quad \forall\, v \in H_0^1(\Omega), \tag{4.1}$$

where, as in Sec. 3.2, the source term is defined as $F(v) = \int_\Omega fv dV$, for a given function $f \in L^2(\Omega)$, and $b(\cdot;\cdot,\cdot)$ is a semilinear form defined as follows:

$$b(u; v, w) = \int_\Omega \kappa(|\nabla u|^2)\nabla v \cdot \nabla w dV \quad \forall\, u, v, w \in H_0^1(\Omega). \tag{4.2}$$

We assume that the nonlinearity $\kappa : \mathbb{R}^+ \to \mathbb{R}^+$ satisfies the following assumptions.

Assumption 4.1. (Nonlinearity assumptions) The nonlinearity $\kappa : \mathbb{R}^+ \to \mathbb{R}^+$ appearing in (4.2) is assumed to satisfy the following:

(i) $\kappa(\cdot)$ is continuous over $[0, +\infty)$;
(ii) there exist two positive constants k_*, k^* such that:

$$k_*(t - s) \le \kappa(t^2)t - \kappa(s^2)s \le k^*(t - s) \quad \forall\, t > s \ge 0.$$

Among all the functions that satisfy Assumption 4.1, we are particularly interested in the Carreau law

$$\kappa(t) = \eta_\infty + (\eta_0 - \eta_\infty)(1 + \lambda t)^{\frac{p-2}{2}}, \quad t \geq 0, \tag{4.3}$$

with $\eta_0 \geq \eta_\infty > 0, \lambda > 0$ and $p \in (1, 2)$. We recall that a fluid that obeys to a Carreau law is a type of generalized quasi-Newtonian fluid where viscosity depends upon the shear rate. For example, the rheologic behavior of many polymeric fluids or rubber-like liquids are frequently described in engineering literature by the Carreau law.

Nonlinear problems play an important role in applied mathematics, and engineering, and have been extensively used to mathematically model phenomena in a wide range of fields (e.g. biology, fluid dynamics, physics, and materials science). Among all the discretizations techniques developed so far, one of the most employed is the finite element method, including non-conforming approaches as discontinuous Galerkin (DG) methods. Regarding the solution of quasilinear boundary value problems, several finite element methods have been studied so far. For example, Ciarlet *et al.*, in Ref. 50, studied Galerkin methods for approximating the solutions of a class of abstract monotone operator equations in Banach spaces using the approach of Zarantonello[122] and Minty.[98] Finite element error estimates for nonlinear elliptic equations of monotone type in divergence form and with gradient nonlinearity in the principal coefficient are considered in Ref. 48. In 1975, Douglas and Dupont[58] studied a Galerkin method for the nonlinear Dirichlet problems

$$-\nabla \cdot (a(x, u)\nabla u) = f, \tag{4.4}$$

subject to non-homogeneous Dirichlet boundary conditions on the boundary of the (two- or three-dimensional) domain Ω. The proposed Galerkin method is a generalization of the Nitsche's method[101] to nonlinear elliptic equations. Optimal error estimates in the energy and the average norms are established, provided the data are sufficiently smooth. Finite element approximations of general quasilinear elliptic systems are considered in Ref. 53. Further extensions including variational crimes such as numerical integration and polygonal approximation of the domain are considered in Ref. 64, see also Refs. 65 and 63 for the case of discontinuous coefficients. A mixed finite element method is analyzed in Refs. 95 and 96: this method is the extension to quasilinear elliptic problems of that of Raviart and Thomas.[106] A primal hybrid finite element method is also considered in Ref. 97. The extension of the streamline diffusion finite element method to quasilinear equations of second order is provided in Ref. 10. In the last 15 years, the DG finite element method has received a considerable interest for the discretization of nonlinear boundary value problems. The development of DG methods for this class of equations has been stimulated by their computational convenience due to their high degree of locality. Rivière and Wheeler consider a nonlinear diffusion operator of the form (4.4) with $a(x, u) : \Omega \times \mathbb{R} \to \mathbb{R}$ Lipschitz continuous with respect to its second variable.[107] Extensions and improved energy estimates with applications to a single phase flow in porous media are presented in Ref. 108. For the *a priori* error analysis of an h-version local DG finite element approximation of quasilinear elliptic equations in divergence form and non-Newtonian flow problems, we refer to Ref. 41 and Refs. 68 and 69, respectively, see also Refs. 55, 56, 61, 62 and 74 for interior penalty methods for the numerical approximation of non-stationary nonlinear convection–diffusion equations. Houston *et al.*[81] present a class of interior penalty hp-DG finite element methods for the approximation of quasilinear elliptic PDEs. Using the theory of monotone operators,[100] the hp-DG formulations are shown to be well-posed, and *a priori* energy estimates which are optimal with respect to the mesh size, and mildly suboptimal in the polynomial approximation degree are shown. The extension to *a posteriori* error analysis is presented in Ref. 82 where computable bounds on the error are derived in terms of a suitable energy norm. A two-grid hp-DG method for the numerical approximation of strongly monotone second-order quasilinear PDEs has been proposed and analyzed in Ref. 51 where *a priori* and *a posteriori* error analysis is presented. The key idea at the basis of the two-grid method (originally introduced by Xu[119–121]) is that the underlying nonlinear problem is discretized on a coarse finite element space; the resulting "coarse" solution is then exploited as a datum for the (linearized) discretization on the finer space. Therefore, on the finer space only a linear system of equations has to be solved. The convergence analysis of DG approximations to symmetric second-order quasilinear elliptic PDEs in divergence form without requiring the global Lipschitz continuity or uniform monotonicity of the stress tensor is provided by Ortner and Süli in Ref. 102. In the context of finite volume approximations of nonlinear problems see also e.g. Refs. 2 and 27.

4.2. *Discrete problem and convergence*

The aim of this section is to briefly recall the mimetic approximation of (4.1); we refer to Ref. 7 for a more detailed discussion.

Let us consider an admissible partition Ω_h of the domain Ω, as explained in Sec. 2. In order to introduce a mimetic discretization of problem (4.1), we first consider the restriction of the form (4.2) on each element $E \in \Omega_h$, i.e.

$$b^E(u; v, w) = \int_E \kappa(|\nabla u|^2)\nabla v \cdot \nabla w dV \quad \forall\, u, v, w \in H^1(E). \tag{4.5}$$

Observe that, whenever $\varphi \in \mathbb{P}^1(E)$, the local form $b^E(\varphi; \cdot, \cdot)$ can be rewritten as

$$b^E(\varphi; v, w) = \kappa(|\nabla\varphi|^2) \int_E \nabla v \cdot \nabla w dV \quad \forall\, \varphi \in \mathbb{P}^1(E),\ \ \forall\, v, w \in H^1(E).$$

In view of the above relation, an MFD discretization of (4.5) can be obtained once that a suitable discrete approximation of the nonlinear term $\kappa(\cdot)$ and of the integral term $\int_E \nabla v \cdot \nabla w dV$ are available. For the latter, we proceed exactly as in

Sec. 3.2, by introducing the bilinear form (3.3) over the space V_h defined in Sec. 2.2. Therefore, we only have to discuss the MFD discretization of the nonlinear term $\kappa(\cdot)$ within each element $E \in \Omega_h$. Let us introduce the following operator

$$\mathcal{G}_h^E : V_h^E \to \mathbb{R}^+, \quad \mathcal{G}_h^E(u_h) := \frac{a_h^E(u_h, u_h)}{|E|}, \tag{4.6}$$

on each $E \in \Omega_h$. Bearing in mind the fact that the bilinear form (3.3) is a discretization of the term $\int_E \nabla v \cdot \nabla w dV$, the operator (4.6) turns out to be a good candidate to approximate $|\nabla u|^2$ within each element. Indeed,

$$\frac{\int_E |\nabla u|^2 dV}{|E|} \sim \mathcal{G}_h^E(u_{\mathrm{I}}) \quad \forall\, u \in \mathcal{C}^0(\bar{E}) \cap H^1(E),$$

where the local interpolation operator $u_{\mathrm{I}} \in V_h|_E$ is defined according to (2.2) and the symbol $\sim$ stands for approximation. In view of the above discussion, we obtain the following mimetic discretization of the local form (4.5)

$$b_h^E(u_h; v_h, w_h) = \kappa(\mathcal{G}_h^E(u_h)) a_h^E(v_h, w_h) \quad \forall\, u_h, v_h, w_h \in V_h|_E.$$

Then, the discrete formulation of problem (4.1) reads as follows: Find $u_h \in V_h^0$, such that

$$b_h(u_h; u_h, v_h) = F_h(v_h) \quad \forall\, v_h \in V_h^0, \tag{4.7}$$

where

$$b_h(u_h; v_h, w_h) = \sum_{E \in \Omega_h} b_h^E(u_h; v_h, w_h) \quad \forall\, u_h, v_h, w_h \in V_h,$$

and where the right-hand side of problem (4.7) is built as in (3.4).

In Ref. 7 it has been proved that the discrete problem (4.7) is well-posed and that the following convergence result holds provided a suitable approximation property is satisfied. The validity of such assumption will be verified through numerical computations in Sec. 4.3.

Theorem 4.1. *Assume that the following approximation property holds: there exists $\alpha > 0$ so that*

$$\|\kappa(|\nabla v|^2) - \kappa(\mathcal{G}_h^E(v_I))\|_\infty \lesssim h^\alpha \quad \forall\, v \in \mathcal{C}^0(\bar{\Omega}) \cap H^1(\Omega). \tag{4.8}$$

Let $u \in H^2(\Omega) \cap H_0^1(\Omega)$ and $u_h \in V_h^0$ be the solutions of the continuous and discrete problems (4.1) *and* (4.7), *respectively. Then, it holds*

$$\|u_I - u_h\|_{1,h} \lesssim h^{\min(1,\alpha)},$$

where u_I is the interpolation of the exact solution defined as in (2.2).

4.3. *Numerical results*

We propose to solve the nonlinear problem (4.7) via linearization employing the Kačanov method. The *idealized* algorithm (i.e. without any stopping criterion) reads as follows: Given $u_h^{(k)} \in V_h^0$

$$\text{find } u_h^{(k+1)} \in V_h^0 \text{ such that}$$
$$b_h(u_h^{(k)}; u_h^{(k+1)}, v_h) = F_h(v_h) \quad \forall\, v_h \in V_h^0, \ \ k \geq 0.$$

The convergence of the sequence $\{u_h^{(k)}\}_{k\geq 0}$ to the "exact" discrete solution u_h of problem (4.7) is stated in the following result. We refer to Ref. 7 for the proof.

Theorem 4.2. *Let $\{u_h^{(k)}\}_{k\geq 0}$ be the sequence built by the Kačanov method. Then $u_h^{(k)} \to u_h$ in V_h, as $k \to +\infty$.*

Next, we present a numerical example taken from Ref. 7, where we have employed the *feasible* Kačanov method supplemented with a suitable stopping criterion as described in Algorithm 4.1. The reliability of the stopping criterion employed in Algorithm 4.1 is discussed in Ref. 7 where it is also proposed a computable error indicator as a possible alternative strategy to stop the iterative scheme.

We suppose that the nonlinearity $\kappa(\cdot)$ obeys to the Carreau law (4.3), with $\eta_0 = 3$, $\eta_\infty = 1$ and $p = 1.7$. The source term f is selected so that $u(x,y) = x(1-x)y(1-y)(1-2y)\exp(-20((2x-1)^2))$ is the analytical solution of problem (4.7). We test our scheme on the same sequences of grids as the ones considered in Sec. 3.3, and throughout this section we set the tolerance `toll` equal to 10^{-8}.

In Table 2 we report the computed relative errors $\|u_{\mathtt{I}} - u_h\|_{1,h}/\|u_{\mathtt{I}}\|_{1,h}$ measured in the discrete energy norm (2.1) as a function of the refinement level ℓ. The last row of Table 2 also shows the computed convergence rate obtained by the linear regression algorithm. We observe that the error goes at a rate that is slightly better than predicted by our theoretical results given in Theorem 4.1, probably due to some improved convergence rate at the nodes of the mesh.

Algorithm 4.1: *Feasible* Kačanov algorithm

Given the initial guess $u_h^{(0)}$, set `toll`, $k = -1$, $u_h^{(-1)} = u_h^{(0)}$;
while $\|u_h^{(k+1)} - u_h^{(k)}\|_{1,h} \geq$ `toll` **do**
  $k + 1 \leftarrow k$;
  `SOLVE` $b_h(u_h^{(k)}; u_h^{(k+1)}, v_h) = F_h(v_h) \quad \forall\, v_h \in V_h$;
end
`SET` $u_h = u_h^{(k+1)}$;

Table 2. Quasilinear elliptic problem. (Example taken from Ref. 7) Computed relative errors $\|u_I - u_h\|_{1,h}/\|u_I\|_{1,h}$ in terms of the refinement level ℓ.

Refinement level	*Median-type* 1	*Median-type* 2	*Quadrilateral*
$\ell = 1$	2.6147e+0	2.6147e+0	4.0053e−1
$\ell = 2$	1.1489e+0	1.0159e+0	1.7027e−1
$\ell = 3$	4.8404e−1	6.0820e−1	5.5403e−2
$\ell = 4$	1.8830e−1	2.3530e−1	1.6881e−2
$\ell = 5$	5.8092e−2	8.6861e−2	5.7466e−3
Rate	1.5580	1.2843	1.2633

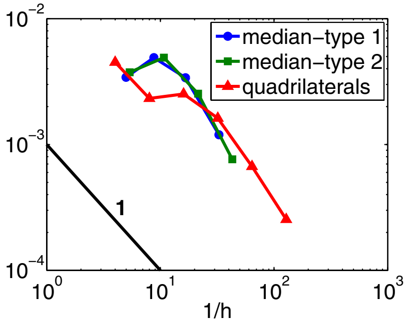

Fig. 3. Quasilinear elliptic problem and numerical validation of assumption (4.8): the behavior of $\|\kappa(\Pi^0|\nabla u|^2) - \kappa(\mathcal{G}_h^E(u_{\mathtt{I}}))\|_{\infty,h}$ vs. $1/h$ (loglog scale) is reported, with u denoting the exact solution.

Finally, we present a numerical approach to validate hypothesis (4.8). Let us introduce the following discrete norm

$$\|v_h\|_{\infty,h} := \sup_{\mathsf{v}\in\mathcal{N}_h} |v_h^{\mathsf{v}}| \quad \forall\, v_h \in V_h,$$

and let us denote with Π^0 the projection onto the space of piecewise constant functions defined on Ω_h. By keeping in mind standard interpolation error estimates, hypothesis (4.8) can be validated by checking the numerical behavior of the following quantity

$$\|\kappa(\Pi^0|\nabla u|^2) - \kappa(\mathcal{G}_h^E(u_{\mathtt{I}}))\|_{\infty,h},$$

where $u_{\mathtt{I}}$ is the interpolation of the exact solution. The numerical results are reported in Fig. 3, from which the value $\alpha = 1$ can be guessed. Then, we can conclude that the optimal parameter α appearing in (4.8) can be set equal to one.

5. Optimal Control Problems

In this section we show the ability of the MFD method to approximate elliptic optimal control problems. To this aim we consider a paradigmatic problem, namely a linear-quadratic elliptic control problem. In Sec. 5.1 we recall the continuous problem, then Sec. 5.2 is devoted to present the MFD discretization and the approximation results and finally Sec. 5.3 presents some numerical results.

5.1. *Problem and literature*

In linear-quadratic elliptic control problems the goal is to drive the solution of a linear elliptic PDE to be close, in the least square sense, to a given function by acting on a control variable (for example, the right-hand side of the differential problem). The *a priori* error analysis of the finite element discretization of this class of problems dates back to the 1970s, in particular to the pioneering works.[59,70] More recently, the subject has seen a great renewal of interest and the literature has considerably grown. For sake of brevity we refer only to the works[9,77,110] and to the recent unified analysis of Ref. 45 (see also the references therein). In particular, in Ref. 45 an abstract result for smooth nonlinear programming problems in Banach space is employed to derive new error estimates under the hypothesis that the state equation is approximated by a finite element scheme, while different discretization methods are used for the control functions. We also mention the *a priori* error analysis performed in Ref. 46 for a mixed finite element approximation of convex optimal control problems.

In contrast to this, *a posteriori* error analysis is quite recent and its origin can be traced back to Ref. 94 where residual-type error estimates have been obtained for distributed convex optimal control problems. Compared to the huge literature on *a posteriori* error estimators for linear problems the existing results for the optimal control problems are rather limited. Among the papers dealing with residual-based *a posteriori* error estimators for elliptic control problems we mention Refs. 76, 79 and 111 and the unified analysis of Ref. 87. Recently, in Ref. 123 a multilevel trust region SQP technique has been combined with an adaptive mesh refinement strategy based on residual *a posteriori* error estimators. Parallelly, quite an effort has been devoted to the study of the dual weighted residual method as an alternative technology to drive adaptive strategies to approximately solve elliptic optimal control problems (see e.g. Refs. 25, 75, 105 and 117).

In the sequel we will focus on the following prototypal problem: Find (F, y, u) such that

$$\begin{cases} \min\limits_{u\in K} \left\{ \dfrac{1}{2}\|y - y^*\|^2_{L^2(\Omega)} + \dfrac{1}{2}\|F - F^*\|^2_{L^2(\Omega)} + \dfrac{\alpha}{2}\|u - u^*\|^2_{L^2(\Omega)} \right\}, \\ F = -\nabla y \quad \text{in } \Omega, \\ \operatorname{div}(F) = f + u \quad \text{in } \Omega, \\ y = 0 \quad \text{on } \partial\Omega, \end{cases} \tag{5.1}$$

where K is a given convex subset of $L^2(\Omega)$, $f, y^*, u^* \in L^2(\Omega)$ and $F^* \in [L^2(\Omega)]^d$ are given functions and α is a positive real number.

We start introducing the variational formulation of problem (5.1) that reads as follows. Find $(F, y, u) \in H(\mathrm{div}, \Omega) \times L^2(\Omega) \times K$ such that

$$\begin{cases} \min_{u \in K} \left\{ \dfrac{1}{2}\|y - y^*\|^2_{L^2(\Omega)} + \dfrac{1}{2}\|F - F^*\|^2_{L^2(\Omega)} + \dfrac{\alpha}{2}\|u - u^*\|^2_{L^2(\Omega)} \right\}, \\ (F, G)_{L^2(\Omega)} - (y, \mathrm{div}(G))_{L^2(\Omega)} = 0 \quad \forall G \in H(\mathrm{div}, \Omega), \\ (\mathrm{div}(F), q)_{L^2(\Omega)} = (f + u, q)_{L^2(\Omega)} \quad \forall q \in L^2(\Omega). \end{cases}$$

It is well known (see e.g. Ref. 89) that the above problem admits a unique solution $(F, y, u) \in H(\mathrm{div}, \Omega) \times L^2(\Omega) \times K$ if and only if there exists $(P, z) \in H(\mathrm{div}, \Omega) \times L^2(\Omega)$ such that $(F, y, P, z, u) \in H(\mathrm{div}, \Omega) \times L^2(\Omega) \times H(\mathrm{div}, \Omega) \times L^2(\Omega) \times K$ satisfies the following optimality conditions:

$$\begin{cases} (F, G)_{L^2(\Omega)} - (y, \mathrm{div}(G))_{L^2(\Omega)} = 0 & \forall G \in H(\mathrm{div}, \Omega), \\ (\mathrm{div}(F), q)_{L^2(\Omega)} = (f + u, q)_{L^2(\Omega)} & \forall q \in L^2(\Omega), \\ (P, G)_{L^2(\Omega)} - (z, \mathrm{div}(G))_{L^2(\Omega)} = -(F - F^*, G)_{L^2(\Omega)} & \forall G \in H(\mathrm{div}, \Omega), \\ (\mathrm{div}\, P, q)_{L^2(\Omega)} = (y^* - y, q)_{L^2(\Omega)} & \forall q \in L^2(\Omega), \\ (\alpha(u - u^*) - z, w - u)_{L^2(\Omega)} \geq 0 & \forall w \in K. \end{cases} \tag{5.2}$$

5.2. *Discrete problem and convergence*

Let X_h and Q_h be defined as in Sec. 2, and suppose that $K_h \subseteq Q_h$ is a closed subset of Q_h; then the discrete formulation of problem (5.2) is easily obtained as follows: Find $(F_h, y_h, P_h, z_h, u_h) \in X_h \times Q_h \times X_h \times Q_h \times K_h$ such that

$$\begin{cases} [F_h, G_h]_{X_h} - [y_h, \mathcal{DIV}_h(G_h)]_{Q_h} = 0 & \forall G_h \in X_h, \\ [\mathcal{DIV}_h(F_h), \boldsymbol{q}]_{Q_h} = [f_{\mathrm{I}} + u_h, q_h]_{Q_h} & \forall q_h \in Q_h, \\ [P_h, G_h]_{X_h} - [z_h, \mathcal{DIV}_h(G_h)]_{Q_h} = -[F_h - F^*_{\mathrm{I}}, G_h]_{X_h} & \forall G_h \in X_h, \\ [\mathcal{DIV}_h(P_h), \boldsymbol{q}]_{Q_h} = [y^*_{\mathrm{I}} - y_h, q_h]_{Q_h} & \forall q_h \in Q_h, \\ [\alpha(u_h - u^*_{\mathrm{I}}) - z_h, w_h - u_h]_{Q_h} \geq 0 & \forall w_h \in K_h, \end{cases} \tag{5.3}$$

where $f_{\mathrm{I}}, y^*_{\mathrm{I}}, F^*_{\mathrm{I}}$ and of u^*_{I} are the interpolation of f, y^*, F^* and of u^*, respectively, defined according to (2.5) and (2.7), and $\mathcal{DIV}_h$ is the discrete divergence operator defined in (2.8). Moreover, we can state the following *a priori* error estimates for the MFD discretization of problem (5.2) which has been proved in Ref. 6.

Theorem 5.1. *Let* $(F, y, P, z, u) \in X \times Q \times X \times Q \times K$ *be the exact optimal solution to* (5.2) *and let* $(F_h, y_h, P_h, z_h, u_h) \in X_h \times Q_h \times X_h \times Q_h \times K_h$ *be the discrete optimal solution to* (5.3)*. Then,*

$$\|u_I - u_h\|_{Q_h} \lesssim h,$$

where $u_I \in Q_h$ is the projection of u as defined in (2.5) *and*

$$\|F_I - F_h\|_{X_h} + \|y_I - y_h\|_{Q_h} \lesssim h,$$
$$\|P_I - P_h\|_{X_h} + \|z_I - z_h\|_{Q_h} \lesssim h,$$

where $y_I, z_I \in Q_h$ are the projection of y and z, respectively, defined as in (2.5), *and $F_I, P_I \in X_h$ are the interpolants of F and P, respectively, defined according to* (2.7).

We recall that the above estimates can be extended analogously to high-order MFD method (see Ref. 6).

5.3. *Numerical results*

The numerical example presented in this section has been performed on the *quadrilateral*, *median-type* 1 and *median-type* 1 decompositions of the domain $\Omega = (0,1)^2$ shown in Fig. 2. The optimization problem has been solved numerically by using the Primal–Dual strategy and the constant α appearing in the optimality conditions (5.2) has been set equal to 1. We have chosen

$$y^* = (1 - 2\pi^2)y, \quad F^* = -\nabla y, \quad u^* = \exp(x_1^2 + x_2^2)\sin(5\pi x_1) + \sin(5\pi x_2),$$

and $f = -\Delta y - u$, so that the exact solution (F, y, P, z, u) of problem (5.2) is given by:

$$y = \sin(\pi x_1)\sin(\pi x_2), \quad z = -\sin(\pi x_1)\sin(\pi x_2), \quad u = \max(u^* + z, 0),$$
$$F = -\nabla y, \quad P = -\nabla z.$$

In Fig. 4 (loglog scale) we report the errors $\|y_{\mathrm{I}} - y_h\|_{Q_h}$, $\|z_{\mathrm{I}} - z_h\|_{Q_h}$, $\|u_{\mathrm{I}} - u_h\|_{Q_h}$ computed in the discrete energy norm defined in (2.4) versus $1/h$. We can observe that the errors of the primal and the dual variables y and z go to zero quadratically, whereas for the control variable z we observe a convergence rate equal to 3/2 as the mesh size h goes to zero. Moreover, let us recall that the error estimates given in Theorem 5.1 predict a linear convergence rate for all of the variables, while the

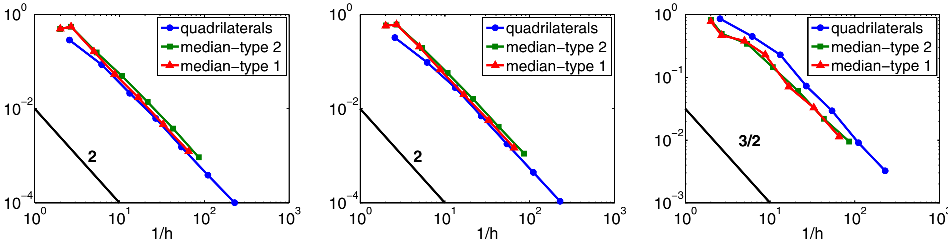

(a) $\|y_{\mathrm{I}} - y_h\|_{Q_h}$ (b) $\|z_{\mathrm{I}} - z_h\|_{Q_h}$ (c) $\|u_{\mathrm{I}} - u_h\|_{Q_h}$

Fig. 4. Optimal control problem. Computed errors $\|y_{\mathrm{I}} - y_h\|_{Q_h}$, $\|z_{\mathrm{I}} - z_h\|_{Q_h}$, $\|u_{\mathrm{I}} - u_h\|_{Q_h}$ vs. $1/h$ (loglog scale).

computed rates seem to be at least half-order better than predicted. For a similar problem in the finite element context, such a superconvergence phenomenon has already been observed in Ref. 46, where a proof of this behavior for the case of the lowest-order Raviart–Thomas elements is presented.

6. Towards a Real Industrial Problem: The Extrusion Process

Many problems in mechanical engineering and physics are mathematically modeled by PDEs defined on domains which are not known *a priori*. The boundaries of these domains are called free boundaries and must be determined as part of the solution. This means that the problem, named *free-boundary problem*, apart from the usual unknown quantities (e.g. velocity, pressure), contains additional geometrical unknowns. A technologically and industrially important category of such free-boundary problems is formed by the viscous free-boundary flow problems, which occurs, for example, in polymer or rubber extrusion.

In the extrusion process the solid material is heated beyond the melting point to be enough malleable. Then, the material is forced by one or more screws through a special die to produce a continuous manufactured item (see Fig. 5). With such a manufacturing process, it is possible to obtain, for example, sheets, films, pipes, sections, layers and slabs. The main problem linked to extrusion is the *die swell* phenomenon which is the increase of the cross-section of the material when it leaves the die (see Fig. 6).

In the following, we briefly discuss a simplified mathematical model of the extrusion process that has been employed in Ref. 8. Let $\Omega \subset \mathbb{R}^2$ be the computational domain. Let us consider $\Omega_1, \Omega_2 \subset \Omega$ such that $\Omega_2 = \Omega \backslash \bar{\Omega}_1$. The region Ω_1 (the so-called *barrel*) includes the extrusion die, while Ω_2 includes the free surface (see

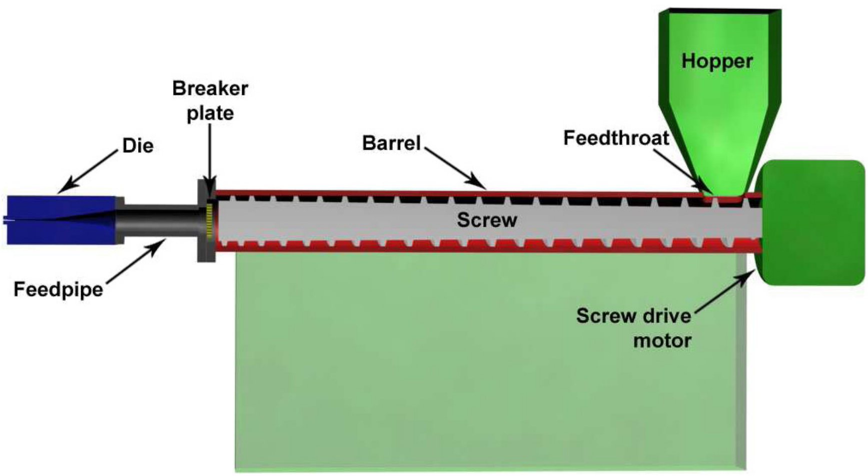

Fig. 5. Extrusion process outline.

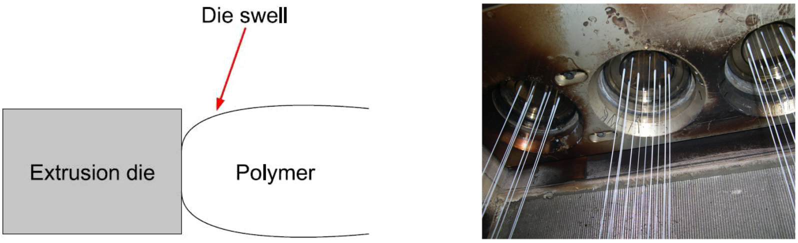

(a) sketch of an horizontal extruder (b) Picture of a vertical polymeric extruder (Courtesy of RadiciYarn s.p.a.)

Fig. 6. *Die swell* phenomenon.

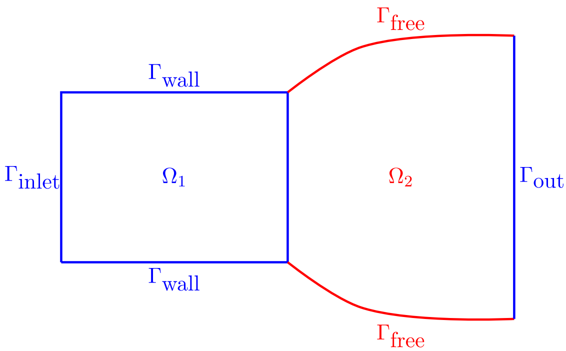

Fig. 7. Two-dimensional sketch of the boundary conditions.

Fig. 7). The flow is modeled as non-Newtonian, incompressible, steady and isothermal. More precisely, the stationary extrusion process is described by the following free-boundary problem: Find the free surface Γ_{free}, the velocity $\mathbf{u}$ and the pressure p such that

$$\begin{cases} \mathbf{div}\,\mathbf{T}(\mathbf{u},p) = \mathbf{0} & \text{in } \Omega, \\ \operatorname{div} \mathbf{u} = 0 & \text{in } \Omega, \\ \mathbf{u} = \mathbf{u}_d & \text{on } \Gamma_{\text{inlet}} \cup \Gamma_{\text{wall}}, \\ \mathbf{u} \cdot \mathbf{n} = 0 & \text{on } \Gamma_{\text{free}}, \\ \mathbf{T}(\mathbf{u},p) \cdot \mathbf{n} = 0 & \text{on } \Gamma_{\text{out}} \cup \Gamma_{\text{free}}, \end{cases} \tag{6.1}$$

where $\mathbf{T}(\mathbf{u},p) = \kappa(|\boldsymbol{\epsilon}(\mathbf{u})|)\boldsymbol{\epsilon}(\mathbf{u}) - p\mathbf{I}$ is the stress tensor, $\boldsymbol{\epsilon}(\mathbf{u}) = (\nabla\mathbf{u} + \nabla\mathbf{u}^T)/2$ is the strain tensor and $|\boldsymbol{\epsilon}(\mathbf{u})|$ is the shear rate. As a consequence of the non-Newtonian nature of the flow, the viscosity $\kappa(\cdot)$ depends on the shear rate $|\boldsymbol{\epsilon}(\mathbf{u})|$. Some of the most common models employed in the literature (e.g. Carreau law and Cross model) will be considered in Sec. 6.1.

Finally, we denote by $\mathbf{n}$ the outer normal vector and define $\mathbf{u}_d$ as follows:

$$\mathbf{u}_d = \begin{cases} \mathbf{u}_{\text{inlet}} & \text{on } \Gamma_{\text{inlet}}, \\ \mathbf{0} & \text{on } \Gamma_{\text{wall}}. \end{cases} \tag{6.2}$$

We remark that on Γ_{free} two boundary conditions are simultaneously imposed; this explains why Γ_{free} (the free-boundary) is part of the unknowns.

In the rest of this section, we will shortly present two very recent lines of investigation naturally stemming from the aim of assembling and testing the main building blocks to perform, in the near future, the MFD numerical simulation of the extrusion process described above. To be more specific, in Sec. 6.1 we will address the approximation of nonlinear Stokes equations, while in Sec. 6.2 we will study the numerical solution of a simple free-boundary elliptic problem. The latter will be first recast as a shape optimization problem, i.e. a control problem where the control variable is represented by the computational domain. In parallel to this, we will also explore the capability of the MFD method to deal with very general polygonal decomposition by considering the mimetic approximation of some other simple, but paradigmatic, shape optimization problems.

6.1. *Nonlinear Stokes problems*

In this subsection, we briefly describe the numerical performance of the MFD method for the approximate solution of nonlinear Stokes problems. In particular, we will consider two different non-Newtonian fluids; the first one governed by the Carreau law and the latter by the Cross model.

Carreau law. We address the solution of the following nonlinear Stokes problem:

$$\begin{cases} -\mathbf{div}\, \mathbf{T}(\mathbf{u}, p) = \mathbf{f} & \text{in } \Omega, \\ \operatorname{div} \mathbf{u} = 0 & \text{in } \Omega, \\ \mathbf{u} = 0 & \text{on } \partial\Omega, \end{cases} \tag{6.3}$$

where $\mathbf{T}(\mathbf{u}, p) = \kappa(|\boldsymbol{\epsilon}(\mathbf{u})|^2)\boldsymbol{\epsilon}(\mathbf{u}) - p\mathbf{I}$ and the nonlinear function $\kappa(\cdot)$ obeys the *Carreau law*, i.e.

$$\kappa(|\epsilon(\mathbf{u})|^2) = \eta_\infty + (\eta_0 - \eta_\infty)(1 + \lambda|\epsilon(\mathbf{u})|^2)^{\frac{p-2}{2}},$$

with $\eta_0 \geq \eta_\infty > 0, \lambda > 0$ and $p \in (1, 2)$. The above nonlinear Stokes problem (6.3) is approximated by resorting to the Uzawa's iterative method which requires the solution of a quasilinear elliptic problem at each iteration. The latter is addressed by employing the MFD method that is an extension of the scheme in Sec. 4. Without addressing the details, we just mention that we search for $u_h \in [V_h]^2$ and $p_h \in Q_h$.

In the following, we present a numerical example taken from Ref. 51 where the nonlinearity is set equal to the Carreau law with the following parameters:

$\eta_\infty = 1, \eta_0 = 2, \lambda = 1$ and $p = 1.2$. We set $\Omega = (0,1)^2$ and we choose the forcing term $\mathbf{f}$ in such a way that the exact solution of (6.3) is

$$\mathbf{u} = \left[\left(1 - \cos\left(\frac{2\pi(e^{px}-1)}{e^p - 1}\right)\right)\sin(2\pi y), \right.$$
$$\left. -pe^{px}\sin\left(\frac{2\pi(e^{px}-1)}{e^p-1}\right)\frac{1-\cos(2\pi y)}{e^p-1}\right],$$
$$p = 2\pi p e^{px}\sin\left(\frac{2\pi(e^{px}-1)}{e^p-1}\right)\frac{\sin(2\pi y)}{e^p-1}.$$

We run the numerical test on the set of meshes depicted in Fig. 2. The computed errors $\|p_{\mathtt{I}} - p_h\|_{Q_h}$ and $\|\mathbf{u}_{\mathtt{I}} - \mathbf{u}_h\|_{1,h}$ versus the mesh size h are reported in Fig. 8. Here, $(\mathbf{u}_h, p_h)$ denotes the exact discrete solution, $(p_{\mathtt{I}}, \mathbf{u}_{\mathtt{I}})$ are the interpolations of the exact continuous solution defined as in Sec. 2.2, $\|\cdot\|_{1,h}$ is the energy norm defined as in (2.1), and $\|\cdot\|_{Q_h}$ is the mesh-dependent norm introduced in (2.4). We can observe a linear convergence for both variables.

Then, for completeness, we present a numerical example on the unitary square $\Omega = (0,1)^2$ where the exact solution $(\mathbf{u}, p)$ of problem (6.3) is set as follows:

$$\mathbf{u} = [-\cos(2\pi x)\sin(2\pi y) + \sin(2\pi y), \sin(2\pi x)\cos(2\pi y) - \sin(2\pi x)],$$
$$p = 2\pi(\cos(2\pi y) - \cos(2\pi x)).$$

and we choose $\eta_0 = 3, \eta_\infty = 2, \lambda = 1$ and $p = 0$. Strictly speaking, due to the particular choice of the parameter p, the resulting non-Newtonian flow is not governed by a Carreau law.

In Fig. 9 (loglog scale) we report, for the set of computational meshes depicted in Fig. 2, the computed errors $\|p_{\mathtt{I}} - p_h\|_{Q_h}$ and $\|\mathbf{u}_{\mathtt{I}} - \mathbf{u}_h\|_{1,h}$ versus the mesh size h. As before, we can observe that the computed errors go to zero linearly as the mesh size h goes to zero.

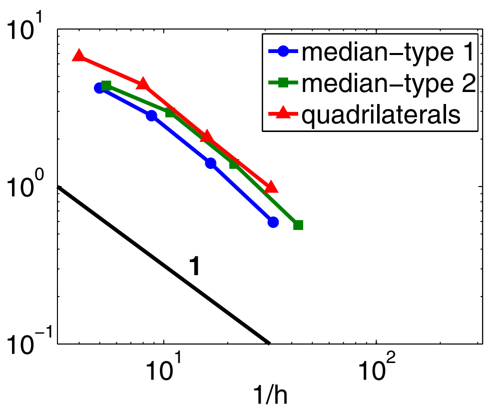

Fig. 8. Nonlinear Stokes problem: MFD discretization of problem (6.3). Computed errors vs. $1/h$.

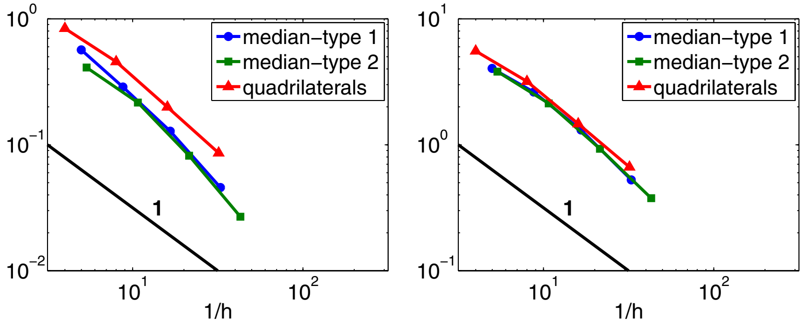

(a) $\|p_{\mathrm{I}} - p_h\|_{Q_h}$ (b) $\|\mathbf{u}_{\mathrm{I}} - \mathbf{u}_h\|_{1,h}$

Fig. 9. Nonlinear Stokes problem: MFD discretization of problem (6.3). Computed errors vs. $1/h$.

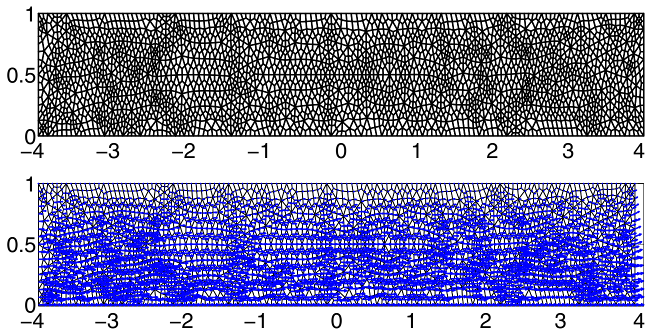

Fig. 10. Nonlinear Stokes problem: MFD discretization of problem (6.4). Computational domain Ω (above) and obtained numerical velocity field (below).

Cross model. We now consider a different non-Newtonian fluid, namely one governed by the Cross model (see (6.5) below). The computational domain corresponds to a simplified barrel (cf. Ω_1 in Fig. 7). In particular, the domain Ω is depicted in Fig. 10 (above). The boundary $\partial\Omega$ is labeled as follows: $\Gamma_{\mathrm{in}} := \{(x, y) : x = -4\}$ and $\Gamma_{\mathrm{out}} = \{(x, y) : x = 4\}$ are the inlet and outlet boundary, respectively, while $\Gamma_s := \{(x, y) : y = 0\}$ and $\Gamma_w := \{(x, y) : y = 1\}$ are the lower and upper part of the channel, respectively.

The nonlinear Stokes problem reads as follows:

$$\begin{cases} \mathbf{div}\, \mathbf{T}(\mathbf{u}, p) = \mathbf{0} & \text{in } \Omega, \\ \operatorname{div} \mathbf{u} = 0 & \text{in } \Omega, \\ \mathbf{u} = \mathbf{u}_d & \text{on } \Gamma_w \cup \Gamma_{\mathrm{in}}, \\ \mathbf{T}(\mathbf{u}, p) \cdot \mathbf{n} = 0 & \text{on } \Gamma_{\mathrm{out}}, \\ \mathbf{u} \cdot \mathbf{n} = 0, \quad (\mathbf{T}(\mathbf{u}, p) \cdot \mathbf{n}) \cdot \mathbf{t} = 0 & \text{on } \Gamma_s, \end{cases} \tag{6.4}$$

Table 3. Parameter of the Cross model (6.5) (taken from Ref. 8).

Parameter	Value
η_0	162.18
η_∞	0
λ	0.0003244
p	0.9493

where $\mathbf{T}(\mathbf{u},p) := \kappa(|\boldsymbol{\epsilon}(\mathbf{u})|)\epsilon(\mathbf{u}) - p\mathbf{I}$ and the nonlinear function κ has been chosen equal to the *Cross model*

$$\kappa(|\boldsymbol{\epsilon}(\mathbf{u})|) := \eta_\infty + \frac{\eta_0 - \eta_\infty}{1 + (\lambda|\boldsymbol{\epsilon}(\mathbf{u})|)^p}, \tag{6.5}$$

where the values of the parameters $\eta_0, \eta_\infty, p, \lambda$ reported in Table 3 are representative of a polymeric fluid (see Ref. 8). We set

$$\mathbf{u}_d = \begin{cases} [1-y^2, 0]^T & \text{on } \Gamma_{\text{in}}, \\ 0 & \text{on } \Gamma_w. \end{cases}$$

Note that on Γ_s we enforce an axial-symmetry boundary condition.

In Fig. 10 (below) we report the obtained numerical velocity field.

6.2. *Shape optimization problems*

In this section, we apply the MFD method to solve shape optimization problems of the form:

$$\text{Find } \Omega^* \in \mathcal{U}_{\text{ad}} : \mathcal{J}(\Omega^*, y(\Omega^*)) = \inf_{\Omega \in \mathcal{U}_{\text{ad}}} \mathcal{J}(\Omega, y(\Omega)),$$

where $\mathcal{J}$ is a given cost functional, $\mathcal{U}_{\text{ad}}$ is the set of admissible domains in $\mathbb{R}^2$ and $y(\Omega)$ is the solution of a PDE on Ω (see e.g. Ref. 52 for an introduction to shape optimization). In this context, the crucial issue in obtaining reliable numerical simulations is to correctly handle the deformation of the computational domain that usually requires a massive use of re-meshing techniques to preserve mesh regularity (see e.g. Ref. 99). Here, we show that the MFD method represents a very promising technology to solve shape optimization problems, without resorting to any re-meshing strategy, since the MFD method can naturally deal with meshes made of very general polygons.

In the rest of the section we will address three different problems. The first two are classical shape optimization problems governed by an elliptic equation and a Stokes equation, respectively. The third one is related to the solution of an elliptic free-boundary problem.

Elliptic problem. We consider the benchmark problem introduced in Ref. 54. In particular, we consider the domain $\Omega \subset \mathbb{R}^2$ with $\partial\Omega = \Gamma_f \cup \Sigma_1 \cup \Sigma_2$ as depicted in Fig. 11. Moreover, let D be an open bounded subset of Ω. The set $\mathcal{U}_{\text{ad}}$ of admissible

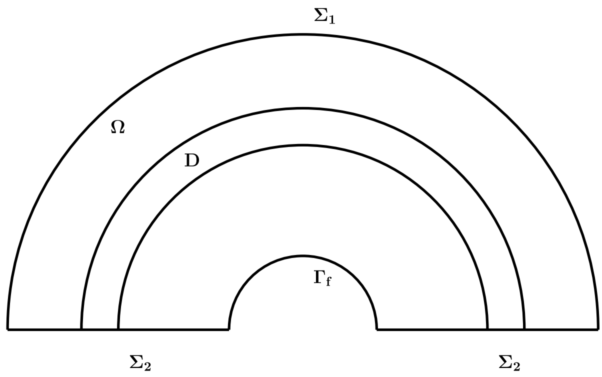

Fig. 11. Computational domain for the optimization problem (6.6) and (6.7).

domains contains all domains obtained through a deformation of Ω by keeping Σ_1 and Σ_2 fixed and by moving only Γ_f in such a way that $\Gamma_f \cap D = \emptyset$. We define the cost functional as follows:

$$\mathcal{J}(\Omega, y(\Omega)) := \frac{1}{2}\int_D (y(\Omega) - z_g)^2 \, dV + \frac{\gamma}{2}\left(\int_{\Gamma_f} dS - P\right)^2, \tag{6.6}$$

where $\gamma > 0$ is a penalization parameter for the length of the moving boundary Γ_f, P is a target value for the perimeter, $z_g : D \to \mathbb{R}$ is a given function and $y(\Omega)$ is the solution of the following elliptic problem on Ω

$$-\Delta y = 0 \quad \text{in } \Omega, \quad y = 0 \quad \text{on } \Sigma_1, \quad \partial_n y = 0 \quad \text{on } \Sigma_2, \quad \partial_n y = 1 \quad \text{on } \Gamma_f. \tag{6.7}$$

Let $\mathbf{x} = (x_1, x_2)$, and let $\|\cdot\|$ denote the Euclidean norm. In the numerical test, we choose the region D equal to the half-ring $\{2 \le \|\mathbf{x}\| \le 2.5\} \cap \{x_2 > 0\}$ and z_g is the exact solution of (6.7) on $\Omega = \{1 < \|\mathbf{x}\| < 3\} \cap \{x_2 > 0\}$. We point out that a global minimizer exists and it is exactly $\Omega^* = \{1 < \|\mathbf{x}\| < 3\} \cap \{x_2 > 0\}$.

In Fig. 12 we report the starting computational domain Ω_0 and the final optimal computational domain obtained after four iterations of a steepest-descent like algorithm (see e.g. Ref. 54 for more details). In the algorithm, we solve problem (6.7) using the mixed MFD method as in Sec. 5.2, see also Refs. 36 and 39. Boundary conditions are suitably modified to include the Neumann term. In Fig. 15 we report the convergence history in terms of the iteration numbers, while in Fig. 13 (right) we can observe the deformation of the elements close to the moving boundary; numerical simulations show that they do not affect the efficiency of the algorithm. Therefore, re-meshing technique seems not to be necessary when using the MFD method for solving shape optimization problems. This issue will be the object of further investigations.

In the sequel, we briefly explore the possibility of incorporating mesh adaptivity into the optimization process (see e.g. Ref. 99 for a similar approach in the FEM

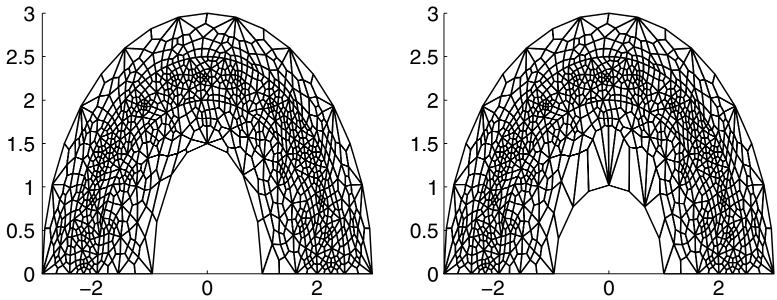

Fig. 12. Shape optimization problem (non-adaptive strategy). Starting computational domain Ω_0 (left) and final one Ω_4 (right) obtained after four iterations.

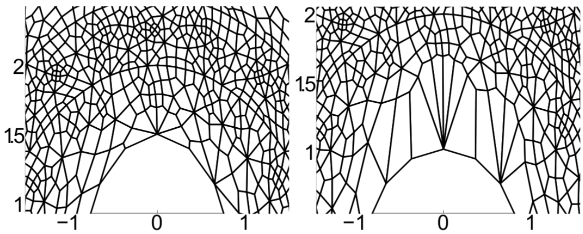

Fig. 13. Shape optimization problem (non-adaptive strategy). Zoom on the elements of the initial domain Ω_0 (left) and the final domain Ω_4 (right). The computational mesh of Ω_4 exhibits distorted elements.

context). To drive the adaptive procedure we employ heuristic indicators, postponing a more rigorous analysis to future works. In particular, we employ the sum of the following two local error indicators:

(η_1) for every polygon $E \subset \Omega_h$ the indicator $\eta_1(E)$ is the local discrete $H^1(E)$ norm of the MFD approximate solution to (6.7);

(η_2) for every polygon $E \subset D$ the indicator $\eta_2(E)$ is the MFD approximation of the quantity $\frac{1}{2}\int_E (y(\Omega) - z_g)^2 \, dV$ and is set to zero outside D.

The local error indicators $(\eta_1 + \eta_2)(E)$ are then employed to mark the elements to be refined, while the marking procedure relies on the Dörfler strategy[57] with marking parameter $\theta = 0.5$. The refinement modulus is the one described in Ref. 3. We decide *a priori* to perform an adaptive refinement step every two iterations of the minimization process. More sophisticated strategies (see e.g. Ref. 99) will be explored in future investigations. In Fig. 14 we report some snapshots of the adaptively refined computational meshes at iteration $n = 0, 2, 4, 6$. Due to the mesh refinement performed close to the movable boundary Γ, the optimal configuration Ω^* results to be more accurately approximated than in the non-adaptive case.

Finally, we compare the performances of the adaptive and non-adaptive strategies. In Fig. 15 we plot the histories of convergence in terms of the functional $J_1 = \frac{1}{2}\int_D (y(\Omega) - z_g)^2 \, dV$, whereas in Table 4 we report the values of J_1 together

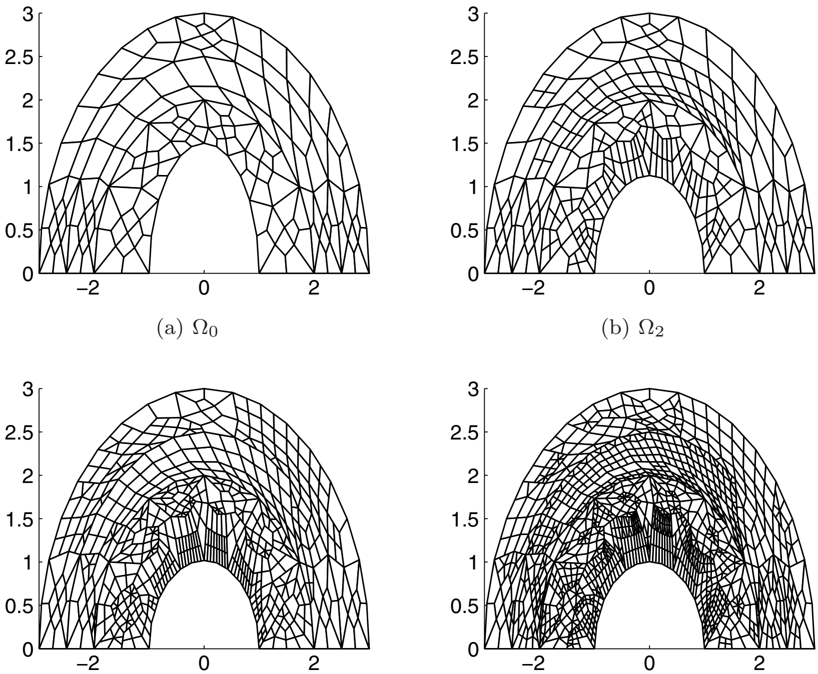

(a) Ω_0 (b) Ω_2

(c) Ω_4 (d) Ω_6

Fig. 14. Shape optimization problem (adaptive strategy). Snapshots of adaptively refined computational meshes at iteration $n = 0, 2, 4, 6$.

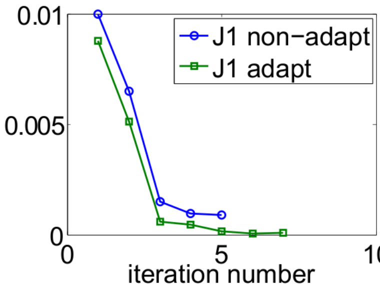

Fig. 15. Shape optimization problem. Comparison of the adaptive and non-adaptive strategies in terms of the convergence history of the functional J_1.

with the employed degrees of freedom. From a close inspection, it is evident that at comparable number of degrees of freedom the adaptive strategy obtains lower values of the cost functional.

Drag minimization. In the second example, we are interested in modeling the flow of a fluid around an obstacle, whose optimal form has to be determined in order to minimize the drag (see e.g. the pioneering works Refs. 103 and 104). Let $\Omega \subset \mathbb{R}^2$ be a bounded domain (channel) as depicted in Fig. 16 (left) where the

Table 4. Adaptive and non-adaptive strategies: Cost functional versus dofs.

	Non-adaptive		Adaptive	
Iteration	Ndofs	J_1	Ndofs	J_1
0	1207	9.990754E−03	157	8.780796E−03
1	1207	6.501192E−03	157	5.103216E−03
2	1207	1.493240E−03	283	5.735032E−04
3	1207	9.618140E−04	283	4.441652E−04
4	1207	8.911968E−04	564	1.368972E−04
5	—	—	564	5.677177E−05
6	—	—	1194	7.538973E−05

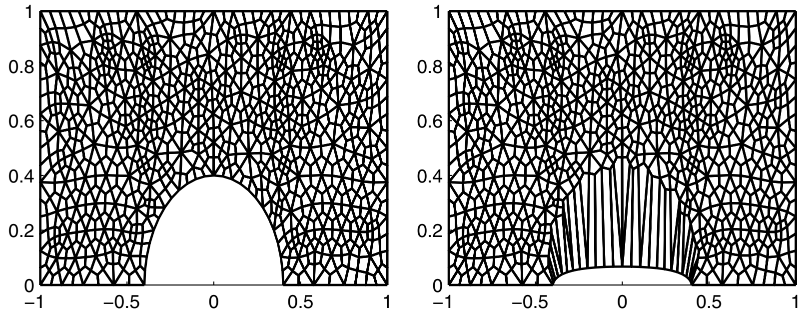

Fig. 16. Drag minimization. Initial configuration of the domain Ω (left), obtained domain (middle) and computed drag versus the number of iteration (right).

obstacle is represented by the half-circle lying on the lower part of the domain and it is denoted by Γ_f. The remaining parts of the boundary are labeled as follows: $\Gamma_{\text{in}} := \{(x, y) : x = -1\}$ and $\Gamma_{\text{out}} := \{(x, y) : x = 1\}$ are the inflow and the outflow layers, respectively while $\Gamma_s := \{(x, y) : y = 0\}$ and $\Gamma_w := \{(x, y) : y = 1\}$ are the lower and upper part of the channel, respectively. The set $\mathcal{U}_{\text{ad}}$ of admissible domains contains all domains obtained through a deformation of Ω by moving only Γ_f and keeping fixed the remaining parts of the boundary.

The fluid flow is modeled by the following linear Stokes problem:

$$\begin{cases} -\text{div}(\mathbf{T}(\mathbf{u}, p)) = 0 & \text{in } \Omega, \\ \text{div}\, \mathbf{u} = 0 & \text{in } \Omega, \\ \mathbf{u} = \mathbf{u}_d & \text{on } \Gamma_w \cup \Gamma_f \cup \Gamma_{\text{in}}, \\ \mathbf{T}(\mathbf{u}, p) \cdot \mathbf{n} = 0 & \text{on } \Gamma_{\text{out}}, \\ \mathbf{u} \cdot \mathbf{n} = 0 (\mathbf{T}(\mathbf{u}, p) \cdot \mathbf{n}) \cdot \mathbf{t} = 0 & \text{on } \Gamma_s, \end{cases} \tag{6.8}$$

where $\mathbf{T}(\mathbf{u}, p) := 2\mu\epsilon(\mathbf{u}) - p\mathbf{I}$ denotes the Cauchy tensor and $\mu = 1$ is the viscosity. We set

$$\mathbf{u}_d = \begin{cases} [1 - y^2 0]^T & \text{on } \Gamma_{\text{in}}, \\ 0 & \text{on } \Gamma_f \cup \Gamma_w. \end{cases}$$

Note that on Γ_s we imposed an axial-symmetry boundary condition while on Γ_w we set a non-slip boundary condition. We choose to minimize the following cost functional:

$$\mathcal{J}(\Omega, \mathbf{u}, p) := -\int_{\Gamma_f} (\mathbf{T}(\mathbf{u}, p)\mathbf{n}) \cdot \widehat{\mathbf{v}}_\infty \, dS + \frac{\lambda}{2}\left(|\Omega_0| - \int_\Omega dx\right)^2, \tag{6.9}$$

where $(\mathbf{u}, p)$ solves (6.8), $\widehat{\mathbf{v}}_\infty = [1, 0]$ is the direction of the fluid and $|\Omega_0|$ is a given target value for the volume. The first term of the functional (6.9) represents the drag of the fluid, while the second one penalizes the volume constraint. In Fig. 16 we plot the initial and final configuration and we report in Fig. 17 the values of the drag $-\int_{\Gamma_f} (\mathbf{T}(\mathbf{u}, p)\mathbf{n}) \cdot \widehat{\mathbf{v}}_\infty \, dS$ versus the number of iterations. We note that the drag decreases along the iterations and the obtained final configuration is in agreement with the so-called *rugby-ball* optimal shape known in Ref. 103.

Free-boundary problem. In the last example, we are interested in solving a free-boundary elliptic problem of the form: Given $\lambda < 0$ and Γ, find the free-boundary $\Gamma_f := \partial\Omega \backslash \bar{\Gamma}$, so that

$$\begin{cases} -\Delta u = 0 & \text{in } \Omega, \\ u = 1 & \text{on } \Gamma, \\ u = 0 & \text{on } \Gamma_f, \\ \dfrac{\partial u}{\partial n} = \lambda & \text{on } \Gamma_f. \end{cases} \tag{6.10}$$

A possible approach to solve (6.10) is to formulate it as a shape optimization problem (see Refs. 73 and 115 for more details). In particular, we aim at minimizing the cost functional

$$\mathcal{J}(\Omega, u) = \int_{\Gamma_f} u^2 dS, \tag{6.11}$$

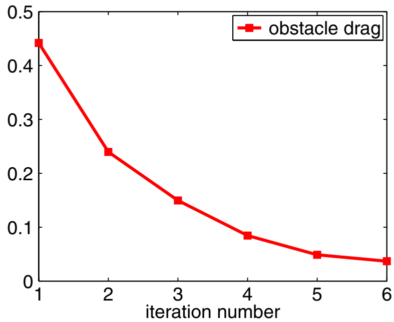

Fig. 17. Drag minimization. Computed drag vs. the number of iteration.

where u solves the following *auxiliary* boundary value problem:

$$\begin{cases} -\Delta u = 0 & \text{in } \Omega, \\ u = 1 & \text{on } \Gamma, \\ \alpha u + \dfrac{\partial u}{\partial n} = \lambda & \text{on } \Gamma_f. \end{cases} \tag{6.12}$$

It is worth noting that the cost functional (6.11) has been chosen in order to incorporate into (6.12) the Dirichlet boundary condition set on Γ_f in the original free-boundary problem (6.10).

The minimization of the functional $\mathcal{J}(\Omega, u)$ is performed over the set $\mathcal{U}_{\text{ad}}$ of admissible configurations Ω obtained by keeping fixed the boundary Γ and deforming only Γ_f (the free-boundary).

As the exact solution of the free-boundary problem (6.10) is zero on Γ_f, the dumping parameter $\alpha > 0$ appearing in (6.12) can be chosen freely. However, following Ref. 115, it turns out that $\alpha = H$, with H being the mean curvature of Γ_f, is a good choice leading in practice to a more robust numerical procedure.

We implement a numerical example originally introduced in Ref. 115. We consider an annular domain, where the fixed boundary is $\Gamma = \{\|\mathbf{x}\| = 1\}$. We choose

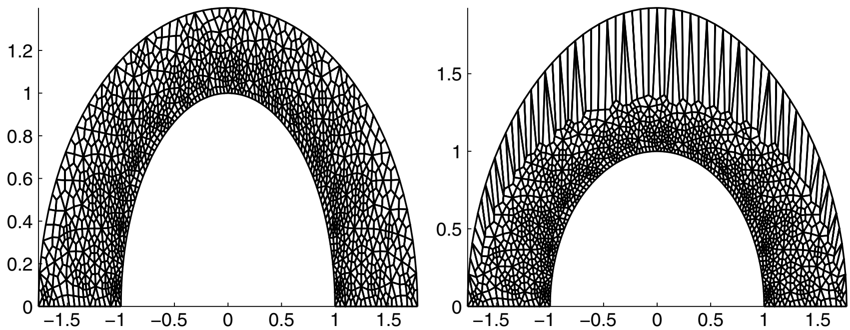

Fig. 18. Free-boundary. Initial (left) and final (right) configuration.

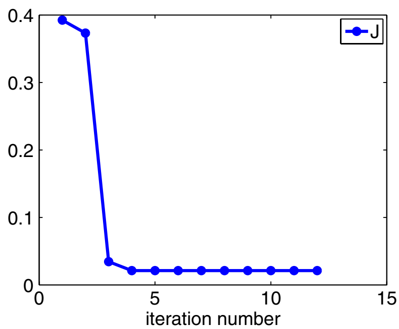

Fig. 19. Free-boundary. Computed functional (6.11) vs. the number of iteration.

$\lambda = -1$ and iteratively solve the problem (6.12) on the half-annulus by imposing proper axial-symmetry boundary conditions on the x-axis (cf. Fig. 18). The initial (non-circular) approximation of the free-boundary Γ_f is depicted in Fig. 18 (left), while the (circular) final configuration is reported in Fig. 18 (right). Finally, in Fig. 19 we plot the value of the functional (6.11) versus the number of total iterations.

7. Conclusions

In this paper we reviewed some recent applications of the MFD method to nonlinear problems (variational inequalities and quasilinear elliptic equations) and constrained control problems governed by linear elliptic PDEs. In all these cases we showed the efficacy of MFDs in building accurate numerical approximations. Moreover, driven by a real-world industrial application, the simulation of the extrusion process, we also presented two very recent lines of investigation naturally stemming from the problems and the techniques considered in this review, namely the impact of the MFD method on the approximate solution of nonlinear Stokes equations and shape optimization/free-boundary problems.

Acknowledgments

P.F.A., L.B.V. and M.V. have been partially supported by the Italian INDAM-GNCS 2013 project "Aspetti emergenti nello studio di strategie adattative per problemi differenziali".

References

1. M. Ainsworth, J. T. Oden and C.-Y. Lee, Local *a posteriori* error estimators for variational inequalities, *Numer. Methods Partial Differential Equations* **9** (1993) 23–33.
2. B. Andreianov, F. Boyer and F. Hubert, Discrete duality finite volume schemes for Leray–Lions-type elliptic problems on general 2D meshes, *Numer. Methods Partial Differential Equations* **23** (2007) 145–195.
3. P. F. Antonietti, L. Beirão da Veiga, C. Lovadina and M. Verani, Hierarchical *a posteriori* error estimators for the mimetic discretization of elliptic problems, *SIAM J. Numer. Anal.* **51** (2013) 654–675.
4. P. F. Antonietti, L. Beirão da Veiga and M. Verani, A mimetic discretization of elliptic obstacle problems, *Math. Comput.* **82** (2013) 1379–1400.
5. P. F. Antonietti, L. Beirão da Veiga and M. Verani, An adaptive MFD method for the obstacle problem, in *Numerical Mathematics and Advanced Applications* (Springer, 2013).
6. P. F. Antonietti, N. Bigoni and M. Verani, Mimetic discretizations of elliptic control problems, *J. Sci. Comput.* **56** (2013) 14–27.
7. P. F. Antonietti, N. Bigoni and M. Verani, Mimetic finite difference approximation of quasilinear elliptic problems, *Calcolo* (2014) 1–23, DOI: 10.1007/s10092-014-0107-y.
8. P. F. Antonietti, N. A. Fadel and M. Verani, Modelling and numerical simulation of the polymeric extrusion process in textile products, *Commun. Appl. Ind. Math.* **1** (2010) 1–13.

9. N. Arada, E. Casas and F. Tröltzsch, Error estimates for the numerical approximation of a semilinear elliptic control problem, *Comput. Optim. Appl.* **23** (2002) 201–229.
10. O. Axelsson, On the numerical solution of convection dominated convection–diffusion problems, in *Problems and Methods in Mathematical Physics*, Teubner-Texte zur Mathematik, Vol. 63 (Teubner, 1984), pp. 8–20.
11. S. Bartels and C. Carstensen, Averaging techniques yield reliable *a posteriori* finite element error control for obstacle problem, *Numer. Math.* **99** (2004) 225–249.
12. L. Beirão da Veiga, A residual-based error estimator for the mimetic finite difference method, *Numer. Math.* **108** (2008) 387–406.
13. L. Beirão da Veiga, A mimetic finite difference method for linear elasticity, *M2AN Math. Model. Numer. Anal.* **44** (2010) 231–250.
14. L. Beirão da Veiga, F. Brezzi, A. Cangiani, G. Manzini, L. D. Marini and A. Russo, Basic principles of virtual element methods, *Math. Models Methods Appl. Sci.* **23** (2013) 199–214.
15. L. Beirão da Veiga, F. Brezzi and L. D. Marini, Virtual elements for linear elasticity problems, *SIAM J. Numer. Anal.* **51** (2013) 794–812.
16. L. Beirão da Veiga, J. Droniou and G. Manzini, A unified approach to handle convection terms in mixed and hybrid finite volumes and mimetic finite difference methods, *IMA J. Numer Anal.* **31** (2011) 1357–1401.
17. L. Beirão da Veiga, V. Gyrya, K. Lipnikov and G. Manzini, Mimetic finite difference method for the Stokes problem on polygonal meshes, *J. Comput. Phys.* **228** (2009) 7215–7232.
18. L. Beirão da Veiga and K. Lipnikov, A mimetic discretization of the Stokes problem with selected edge bubbles, *SIAM J. Sci. Comput.* **32** (2010) 875–893.
19. L. Beirão da Veiga, K. Lipnikov and G. Manzini, Convergence of the mimetic finite difference method for the Stokes problem on polyhedral meshes, *SIAM J. Numer. Anal.* **48** (2010) 1419–1443.
20. L. Beirão da Veiga, K. Lipnikov and G. Manzini, Arbitrary-order nodal mimetic discretizations of elliptic problems on polygonal meshes, *SIAM J. Numer. Anal.* **49** (2011) 1737–1760.
21. L. Beirão da Veiga, K. Lipnikov and G. Manzini, *The Mimetic Finite Difference Method for Elliptic Problems* (Springer, 2014).
22. L. Beirão da Veiga, C. Lovadina and D. Mora, Numerical results for mimetic discretization of Reissner–Mindlin plate problems, *Calcolo* **50** (2013) 209–237.
23. L. Beirão da Veiga and G. Manzini, An *a posteriori* error estimator for the mimetic finite difference approximation of elliptic problems, *Int. J. Numer. Methods Engrg.* **76** (2008) 1696–1723.
24. L. Beirão da Veiga and D. Mora, A mimetic discretization of the Reissner–Mindlin plate bending problem, *Numer. Math.* **117** (2011) 425–462.
25. S. Berrone and M. Verani, A new marking strategy for the adaptive finite element approximation of optimal control constrained problems, *Optim. Methods Softw.* **26** (2011) 747–775.
26. M. Boman, *A posteriori* error analysis in the maximum norm for a penalty finite element method for the time-dependent obstacle problem, preprint, Chalmers FEM Center, Goteborg, Sweden (2001).
27. F. Boyer and F. Hubert, Finite volume method for 2D linear and nonlinear elliptic problems with discontinuities, *SIAM J. Numer. Anal.* **46** (2008) 3032–3070.
28. D. Braess, *A posteriori* error estimators for obstacle problems — another look, *Numer. Math.* **101** (2005) 415–421.

29. D. Braess, C. Carstensen and R. Hoppe, Convergence analysis of a conforming adaptive finite element method for an obstacle problem, *Numer. Math.* **107** (2007) 455–471.
30. H. R. Brezis and G. Stampacchia, Sur la régularité de la solution d'inéquations elliptiques, *Bull. Soc. Math. France* **96** (1968) 153–180.
31. F. Brezzi and A. Buffa, Innovative mimetic discretizations for electromagnetic problems, *J. Comput. Appl. Mech.* **234** (2010) 1980–1987.
32. F. Brezzi, A. Buffa and K. Lipnikov, Mimetic finite differences for elliptic problems, *M2AN Math. Model. Numer. Anal.* **43** (2009) 277–295.
33. F. Brezzi, A. Buffa and G. Manzini, Mimetic scalar products for discrete differential forms, *J. Comput. Phys.* **257** (2014) 1228–1259.
34. F. Brezzi, W. Hager and P. Raviart, Error estimates for the finite element solution of variational inequalities, *Numer. Math.* **28** (1977) 431–443.
35. F. Brezzi, W. Hager and P. Raviart, Error estimates for the finite element solution of variational inequalities (part II mixed methods), *Numer. Math.* **31** (1978/79) 1–16.
36. F. Brezzi, K. Lipnikov and M. Shashkov, Convergence of the mimetic finite difference method for diffusion problems on polyhedral meshes, *SIAM J. Numer. Anal.* **43** (2005) 1872–1896 (electronic).
37. F. Brezzi, K. Lipnikov and M. Shashkov, Convergence of mimetic finite difference method for diffusion problems on polyhedral meshes with curved faces, *Math. Models Methods Appl. Sci.* **16** (2006) 275–297.
38. F. Brezzi, K. Lipnikov, M. Shashkov and V. Simoncini, A new discretization methodology for diffusion problems on generalized polyhedral meshes, *Comput. Methods Appl. Mech. Engrg.* **196** (2007) 3682–3692.
39. F. Brezzi, K. Lipnikov and V. Simoncini, A family of mimetic finite difference methods on polygonal and polyhedral meshes, *Math. Models Methods Appl. Sci.* **15** (2005) 1533–1551.
40. F. Brezzi and L. Marini, Virtual element method for plate bending problems, *Comput. Methods Appl. Mech. Engrg.* **253** (2012) 455–462.
41. R. Bustinza and G. N. Gatica, A local discontinuous Galerkin method for nonlinear diffusion problems with mixed boundary conditions, *SIAM J. Sci. Comput.* **26** (2004) 152–177.
42. A. Cangiani, F. Gardini and G. Manzini, Convergence of the mimetic finite difference method for eigenvalue problems in mixed form, *Comput. Methods Appl. Mech. Engrg.* **200** (2011) 1150–1160.
43. A. Cangiani and G. Manzini, Flux reconstruction and pressure post-processing in mimetic finite difference methods, *Comput. Methods Appl. Mech. Engrg.* **197** (2008) 933–945.
44. A. Cangiani, G. Manzini and A. Russo, Convergence analysis of the mimetic finite difference method for elliptic problems, *SIAM J. Numer. Anal.* **47** (2009) 2612–2637.
45. E. Casas and F. Tröltzsch, A general theorem on error estimates with application to a quasilinear elliptic optimal control problem, *Comput. Optim. Appl.* **53** (2012) 173–206.
46. Y. Chen, Y. Huang, W. Liu and N. Yan, Error estimates and superconvergence of mixed finite element methods for convex optimal control problems, *J. Sci. Comput.* **42** (2010) 382–403.
47. Z. Chen and R. Nochetto, Residual type *a posteriori* error estimates for elliptic obstacle problems, *Numer. Math.* **84** (2000) 527–548.

48. S.-S. Chow, Finite element error estimates for nonlinear elliptic equations of monotone type, *Numer. Math.* **54** (1989) 373–393.
49. P. G. Ciarlet, *The Finite Element Method for Elliptic Problems* (North-Holland, 1978).
50. P. G. Ciarlet, M. H. Schultz and R. S. Varga, Numerical methods of high-order accuracy for nonlinear boundary value problems. V. Monotone operator theory, *Numer. Math.* **13** (1969) 51–77.
51. S. Congreve, P. Houston, E. Suli and T. P. Wihler, Discontinuous Galerkin finite element approximation of quasilinear elliptic boundary value problems. II. Strongly monotone quasi-Newtonian flows, Technical Report NA-11/20, The University of Nottingham (2011).
52. M. C. Delfour and J.-P. Zolésio, *Shapes and Geometries*, 2nd edn., Advances in Design and Control, Vol. 22 (SIAM, 2011).
53. M. Dobrowolski and R. Rannacher, Finite element methods for nonlinear elliptic systems of second order, *Math. Nachr.* **94** (1980) 155–172.
54. G. Doğan, P. Morin, R. H. Nochetto and M. Verani, Discrete gradient flows for shape optimization and applications, *Comput. Methods Appl. Mech. Engrg.* **196** (2007) 3898–3914.
55. V. Dolejší, M. Feistauer and J. Hozman, Analysis of semi-implicit DGFEM for nonlinear convection–diffusion problems on nonconforming meshes, *Comput. Methods Appl. Mech. Engrg.* **196** (2007) 2813–2827.
56. V. Dolejší, M. Feistauer, V. Kučera and V. Sobotíková, An optimal $L^\infty(L^2)$-error estimate for the discontinuous Galerkin approximation of a nonlinear non-stationary convection–diffusion problem, *IMA J. Numer. Anal.* **28** (2008) 496–521.
57. W. Dörfler, A convergent adaptive algorithm for Poisson's equation, *SIAM J. Numer. Anal.* **33** (1996) 1106–1124.
58. J. Douglas, Jr. and T. Dupont, A Galerkin method for a nonlinear Dirichlet problem, *Math. Comput.* **29** (1975) 689–696.
59. R. S. Falk, Approximation of a class of optimal control problems with order of convergence estimates, *J. Math. Anal. Appl.* **44** (1973) 28–47.
60. R. S. Falk, Error estimates for the approximation of a class of variational inequalities, *Math. Comput.* **28** (1974) 963–971.
61. M. Feistauer, V. Dolejší, V. Kučera and V. Sobotíková, $L^\infty(L^2)$-error estimates for the DGFEM applied to convection–diffusion problems on nonconforming meshes, *J. Numer. Math.* **17** (2009) 45–65.
62. M. Feistauer, V. Kučera, K. Najzar and J. Prokopová, Analysis of space-time discontinuous Galerkin method for nonlinear convection–diffusion problems, *Numer. Math.* **117** (2011) 251–288.
63. M. Feistauer and V. Sobotíková, Finite element approximation of nonlinear elliptic problems with discontinuous coefficients, *RAIRO Modél. Math. Anal. Numér.* **24** (1990) 457–500.
64. M. Feistauer and A. Ženíšek, Finite element solution of nonlinear elliptic problems, *Numer. Math.* **50** (1987) 451–475.
65. M. Feistauer and A. Ženíšek, Finite element variational crimes in nonlinear elliptic problems, in *Proc. Second Int. Symp. Numerical Analysis*, Prague, 1987, Teubner-Texte zur Mathematik, Vol. 107 (Teubner, 1988), pp. 28–35.
66. D. French, S. Larsson and R. Nochetto, Pointwise *a posteriori* error analysis for an adaptive penalty finite element method for the obstacle problem, *Comput. Meth. Appl. Math.* **1** (2001) 18–38.

67. A. Friedman, *Variational Principles and Free-Boundary Problems*, Pure and Applied Mathematics (Wiley, 1982).
68. G. N. Gatica, M. González and S. Meddahi, A low-order mixed finite element method for a class of quasi-Newtonian Stokes flows. I. *A priori* error analysis, *Comput. Methods Appl. Mech. Engrg.* **193** (2004) 881–892.
69. G. N. Gatica, M. González and S. Meddahi, A low-order mixed finite element method for a class of quasi-Newtonian Stokes flows. II. *A posteriori* error analysis, *Comput. Methods Appl. Mech. Engrg.* **193** (2004) 893–911.
70. T. Geveci, On the approximation of the solution of an optimal control problem governed by an elliptic equation, *RAIRO Anal. Numér.* **13** (1979) 313–328.
71. V. Gyrya and K. Lipnikov, M-adaptation method for acoustic wave equation on square meshes, *J. Comput. Acoust.* **20** (2012) 1250022, 23 pp.
72. V. Gyrya, K. Lipnikov, I. Arønson and L. Berlyand, Effective shear viscosity and dynamics of suspensions of micro-swimmers at moderate concentrations, *J. Math. Biol.* **65** (2011) 707–740.
73. J. Haslinger, T. Kozubek, K. Kunisch and G. Peichl, Shape optimization and fictitious domain approach for solving free boundary problems of Bernoulli type, *Comput. Optim. Appl.* **26** (2003) 231–251.
74. O. Havle, V. Dolejší and M. Feistauer, Discontinuous Galerkin method for nonlinear convection–diffusion problems with mixed Dirichlet–Neumann boundary conditions, *Appl. Math.* **55** (2010) 353–372.
75. M. Hintermüller and R. H. W. Hoppe, Goal-oriented adaptivity in control constrained optimal control of partial differential equations, *SIAM J. Control Optim.* **47** (2008) 1721–1743.
76. M. Hintermüller, R. H. W. Hoppe, Y. Iliash and M. Kieweg, An *a posteriori* error analysis of adaptive finite element methods for distributed elliptic control problems with control constraints, *ESAIM Control Optim. Calc. Var.* **14** (2008) 540–560.
77. M. Hinze, A variational discretization concept in control constrained optimization: The linear-quadratic case, *Comput. Optim. Appl.* **30** (2005) 45–61.
78. I. Hlaváček, J. Haslinger, J. Nečas and J. Lovíšek, *Solution of Variational Inequalities in Mechanics*, Applied Mathematical Sciences, Vol. 66 (Springer, 1988). Translated from the Slovak by J. Jarník.
79. R. H. W. Hoppe and M. Kieweg, Adaptive finite element methods for mixed control-state constrained optimal control problems for elliptic boundary value problems, *Comput. Optim. Appl.* **46** (2010) 511–533.
80. R. H. W. Hoppe and R. Kornhuber, Adaptive multilevel methods for obstacle problems, *SIAM J. Numer. Anal.* **31** (1994) 301–323.
81. P. Houston, J. Robson and E. Süli, Discontinuous Galerkin finite element approximation of quasilinear elliptic boundary value problems. I. The scalar case, *IMA J. Numer. Anal.* **25** (2005) 726–749.
82. P. Houston, E. Süli and T. P. Wihler, *A posteriori* error analysis of *hp*-version discontinuous Galerkin finite-element methods for second-order quasi-linear elliptic PDEs, *IMA J. Numer. Anal.* **28** (2008) 245–273.
83. P. Jaillet, D. Lamberton and B. Lapeyre, Variational inequalities and the pricing of American options, *Acta Appl. Math.* **21** (1990) 263–289.
84. C. Johnson, Adaptive finite element methods for the obstacle problem, *Math. Models Methods Appl. Sci.* **2** (1992) 483–487.
85. N. Kikuchi, Convergence of a penalty-finite element approximation for an obstacle problem, *Numer. Math.* **37** (1981) 105–120.
86. D. Kinderlehrer and G. Stampacchia, *An Introduction to Variational Inequalities and Their Applications*, Classics in Applied Mathematics, Vol. 31 (SIAM, 2000).

87. K. Kohls, A. Rsch and K. G. Siebert, *A posteriori* error estimators for control constrained optimal control problems, in *Constrained Optimization and Optimal Control for Partial Differential Equations*, Vol. 160, eds. G. Leugering *et al.* (Springer, 2012), pp. 431–443.
88. R. Kornhuber, *A posteriori* error estimates for elliptic variational inequalities, *Comput. Math. Appl.* **31** (1996) 49–60.
89. J.-L. Lions, *Optimal Control of Systems Governed by Partial Differential Equations*, Translated from the French by S. K. Mitter, Grundlehren der Mathematischen Wissenschaften, Band 170 (Springer, 1971).
90. K. Lipnikov, G. Manzini and M. Shashkov, Mimetic finite difference method, *J. Comput. Phys.* **257** (2014) 1163–1227.
91. K. Lipnikov, G. Manzini and D. Svyatskiy, Analysis of the monotonicity conditions in the mimetic finite difference method for elliptic problems, *J. Comput. Phys.* **230** (2011) 2620–2642.
92. K. Lipnikov, G. Manzini and D. Svyatskiy, Monotonicity conditions in the mimetic finite difference method, in *Finite Volumes for Complex Applications VI Problems & Perspectives*, Vol. 1, eds. J. Fořt, J. Fürst, J. Halama, R. Herbin and F. Hubert (Springer, 2011), pp. 653–662.
93. K. Lipnikov, J. Moulton and D. Svyatskiy, A Multilevel Multiscale Mimetic (M^3) method for two-phase flows in porous media, *J. Comput. Phys.* **227** (2008) 6727–6753.
94. W. Liu and N. Yan, *A posteriori* error estimates for distributed convex optimal control problems, *Adv. Comput. Math.* **15** (2001) 285–309.
95. F. A. Milner, *Mixed Finite Element Methods of Quasilinear Second-Order Elliptic Problems* (ProQuest LLC, 1983).
96. F. A. Milner, Mixed finite element methods for quasilinear second-order elliptic problems, *Math. Comput.* **44** (1985) 303–320.
97. F. A. Milner, A primal hybrid finite element method for quasilinear second order elliptic problems, *Numer. Math.* **47** (1985) 107–122.
98. G. J. Minty, Monotone (nonlinear) operators in Hilbert space, *Duke Math. J.* **29** (1962) 341–346.
99. P. Morin, R. Nochetto, M. Pauletti and M. Verani, Adaptive finite element method for shape optimization, *ESAIM Control, Optim. Calc. Var.* **18** (2012) 1122–1149.
100. J. Nečas, *Introduction to the Theory of Nonlinear Elliptic Equations* (Wiley, 1986). Reprint of the 1983 edition.
101. J. Nitsche, Über ein variationsprinzip zur lösung von Dirichlet-problemen bei verwendung von teilräumen, die keinen randbedingungen unterworfen sind, *Abh. Math. Sem. Univ. Hamburg* **36** (1971) 9–15. Collection of articles dedicated to Lothar Collatz on his sixtieth birthday.
102. C. Ortner and E. Süli, Discontinuous Galerkin finite element approximation of nonlinear second-order elliptic and hyperbolic systems, *SIAM J. Numer. Anal.* **45** (2007) 1370–1397.
103. O. Pironneau, On optimum profiles in Stokes flow, *J. Fluid Mech.* **59** (1973) 117–128.
104. O. Pironneau, On optimum design in fluid mechanics, *J. Fluid Mech.* **64** (1974) 97–110.
105. R. Rannacher and B. Vexler, Adaptive finite element discretization in PDE-based optimization, *GAMM–Mitt.* **33** (2010) 177–193.
106. P.-A. Raviart and J. M. Thomas, A mixed finite element method for second-order elliptic problems, in *Mathematical Aspects of Finite Element Methods*, Lecture Notes in Mathematics, Vol. 606 (Springer, 1977), pp. 292–315.

107. B. Rivière and M. F. Wheeler, A discontinuous Galerkin method applied to nonlinear parabolic equations, in *Discontinuous Galerkin Methods*, Lecture Notes in Computational Science and Engineering, Vol. 11 (Springer, 2000), pp. 231–244.
108. B. Rivière, M. F. Wheeler and V. Girault, *A priori* error estimates for finite element methods based on discontinuous approximation spaces for elliptic problems, *SIAM J. Numer. Anal.* **39** (2001) 902–931.
109. J.-F. Rodrigues, *Obstacle Problems in Mathematical Physics*, North-Holland Mathematics Studies, Vol. 134 (North-Holland, 1987). Notas de Matemática [Mathematical Notes], Vol. 114.
110. A. Rösch, Error estimates for linear-quadratic control problems with control constraints, *Optim. Methods Softw.* **21** (2006) 121–134.
111. A. Rösch and D. Wachsmuth, *A-posteriori* error estimates for optimal control problems with state and control constraints, *Numer. Math.* **120** (2012) 733–762.
112. R. Scholz, Numerical solution of the obstacle problem by the penalty method, *Computing* **32** (1984) 297–306.
113. R. Scholz, Numerical solution of the obstacle problem by the penalty method. II. Time-dependent problems, *Numer. Math.* **49** (1986) 255–268.
114. K. G. Siebert and A. Veeser, A unilaterally constrained quadratic minimization with adaptive finite elements, *SIAM J. Optim.* **18** (2007) 260–289 (electronic).
115. T. Tiihonen, Shape optimization and trial methods for free boundary problems, *RAIRO Modél. Math. Anal. Numér.* **31** (1997) 805–825.
116. A. Veeser, Efficient and reliable *a posteriori* error estimators for elliptic obstacle problems, *SIAM J. Numer. Anal.* **39** (2001) 146–167 (electronic).
117. B. Vexler and W. Wollner. Adaptive finite elements for elliptic optimization problems with control constraints, *SIAM J. Control Optim.* **47** (2008) 509–534.
118. L.-H. Wang, On the quadratic finite element approximation to the obstacle problem, *Numer. Math.* **92** (2002) 771–778.
119. J. Xu, A new class of iterative methods for non-self-adjoint or indefinite problems, *SIAM J. Numer. Anal.* **29** (1992) 303–319.
120. J. Xu, A novel two-grid method for semilinear elliptic equations, *SIAM J. Sci. Comput.* **15** (1994) 231–237.
121. J. Xu, Two-grid discretization techniques for linear and nonlinear PDEs, *SIAM J. Numer. Anal.* **33** (1996) 1759–1777.
122. E. H. Zarantonello, *Solving Functional Equations by Contractive Averaging* (Mathematics Research Center, 1960).
123. J. C. Ziems and S. Ulbrich, Adaptive multilevel inexact SQP methods for PDE-constrained optimization, *SIAM J. Optim.* **21** (2011) 1–40.
124. Q. Zou, A. Veeser, R. Kornhuber and C. Gräser, Hierarchical error estimates for the energy functional in obstacle problems, *Numer. Math.* **117** (2011) 653–677.